addition to hair anomalies, he did not show any other associated findings. Both the parents were unaffected and there were no consanguinities between them.

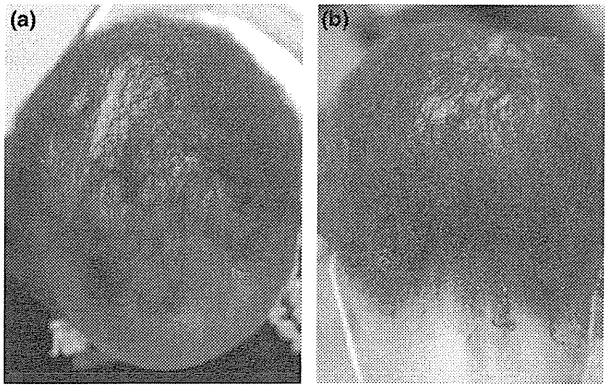

Figure 1. Clinical features of the patient. In addition to woolly hair, he showed sparse hair especially on frontal, (a) parietal and (b) occipital regions of the scalp.

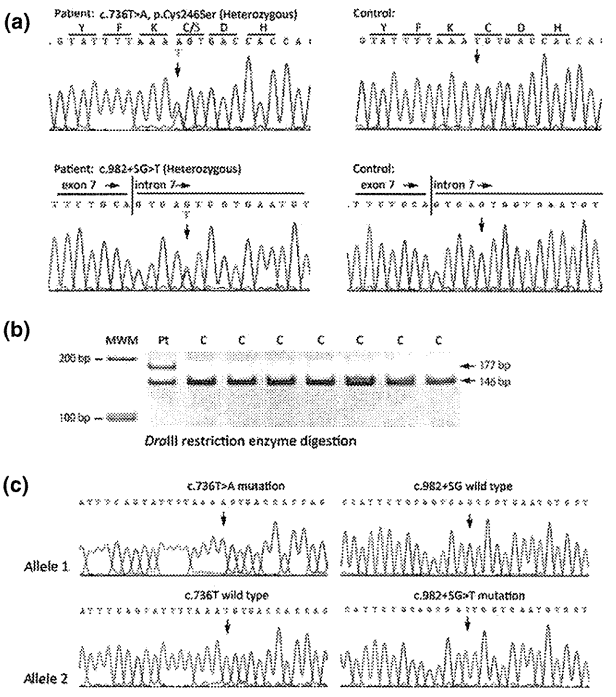

Figure 2. Identification of compound heterozygous mutations in the *LIPH* gene. (a) The patient was heterozygous for the mutations c.736T>A (top panel) and c.982+5G>T (bottom panel). (b) Screening assay for the mutation c.982+5G>T with the restriction enzyme *Dra*III. Polymerase chain reaction products from the wild-type allele (177 bp) were digested into 146-bp and 31-bp fragments, while those from the mutant allele were undigested. The 31-bp fragments are not shown. C, control individuals; MWM, molecular weight markers; Pt, patient. (c) Results of direct sequencing of each mutant allele that was cloned into the pCRII-TOPO vector.

Mutation analysis of the *LIPH* gene

After obtaining informed consent, we collected peripheral blood samples from the patient and 100 population-matched unrelated healthy control individuals (under institutional approval and in adherence to the principles of the Declaration of Helsinki). Genomic DNA was isolated from these samples according to standard techniques. We were unable to obtain samples from either parent of the patient, because they were reluctant to give permission. Using the genomic DNA from the patient, polymerase chain reaction (PCR) and direct sequencing analysis of the *LIPH* gene were performed following the methods described previously.[3]

To screen for the mutation c.982+5G>T, a part of exon 7 and intron 7 of the *LIPH* gene was PCR amplified using a mismatch forward primer (5′-ACACAGCTGAGGAGAGCCCATT CTGCA**C**TG-3′) and a reverse primer (5′-GTAGACTCAGGAGT CAACCG-3′). Note that the G>C substitution was introduced into the forward primer to generate a restriction enzyme site of *Dra*III only in the PCR product amplified from the wild-type allele (shown in bold and underlined). The PCR products were digested by *Dra*III at 37°C for 3 h, and analyzed on 7.5% polyacrylamide gels.

In order to investigate if the mutations c.736T>A and c.982+5G>T were located on different alleles, a long PCR was performed using a forward primer (5′-CAGGGCCAGATGAG AAATTGTGT-3′) and a reverse primer (5′-TGCCAAGAAGTAGC

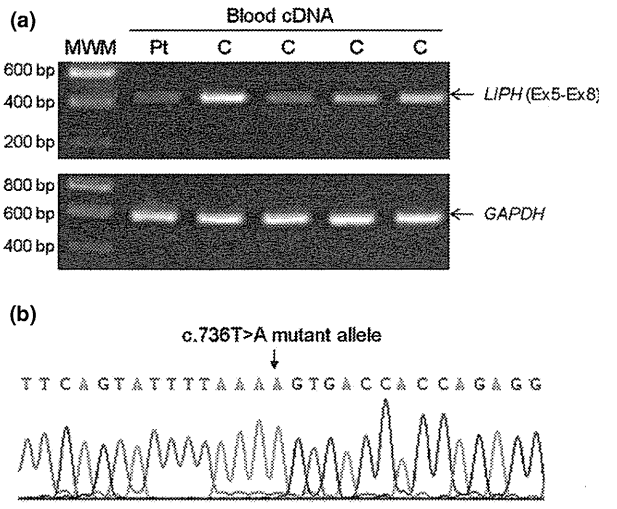

Figure 3. Results of reverse transcription polymerase chain reaction (RT–PCR). (a) Using blood-derived RNA from the patient and control individuals, RT–PCR for the *LIPH* gene was performed. In PCR for the *LIPH* transcripts, a single fragment, 417 bp in size, was amplified from all the samples, but the amplification efficiency appeared to be different even between the control samples. *GAPDH* cDNA was used as a positive control. C, control individuals; MWM, molecular weight markers; Pt, patient. (b) Direct sequencing of the RT–PCR product of the patient revealed the *LIPH* transcript only from the c.736T>A allele, suggesting degradation of that from the c.982+5G>T allele.

CAGGAAGC-3′) so that the PCR products included the sequences of both mutations. The PCR products were TA-cloned into the pCRII-TOPO vector (Invitrogen, Carlsbad, CA, USA), and then each allele was separately sequenced.

Reverse transcription (RT)–PCR and *in vitro* transcription assay

Total RNA was extracted from blood samples of the patient and healthy control individuals using ISOGEN-LS (NIPPON GENE, Tokyo, Japan). One microgram of total RNA was reverse transcribed with oligo-dT primers and Superscript III (Invitrogen). Using the first-strand cDNA as a template, the *LIPH* cDNA was PCR amplified using a forward primer (LIPH-5F4: 5′-TACCCAAATGGAGGATTGGATC-3′) and a reverse primer (LIPH-8R3: 5′-GGATTCTGTGGTGTTTCCAGC-3′), which were designated in exons 5 and 8 of the *LIPH* gene, respectively. The PCR products were run on 1% agarose gels, and were directly sequenced.

Using the genomic DNA of the patient as a template, a part of the *LIPH* gene, including the sequences between exons 6 and 8, was amplified by PCR using a forward primer (5′-CAC TTGCCAGCATGAATTCTTATC-3′) and a reverse primer (5′-AA AAGGTACCCTGGGAGATCAAGAACCAGG-3′). The PCR products were subsequently cloned into *Eco*RI and *Kpn*I sites of the mammalian expression vector pCXN2.1.[24] The vectors were transfected into HEK293T cells with Lipofectamine 2000

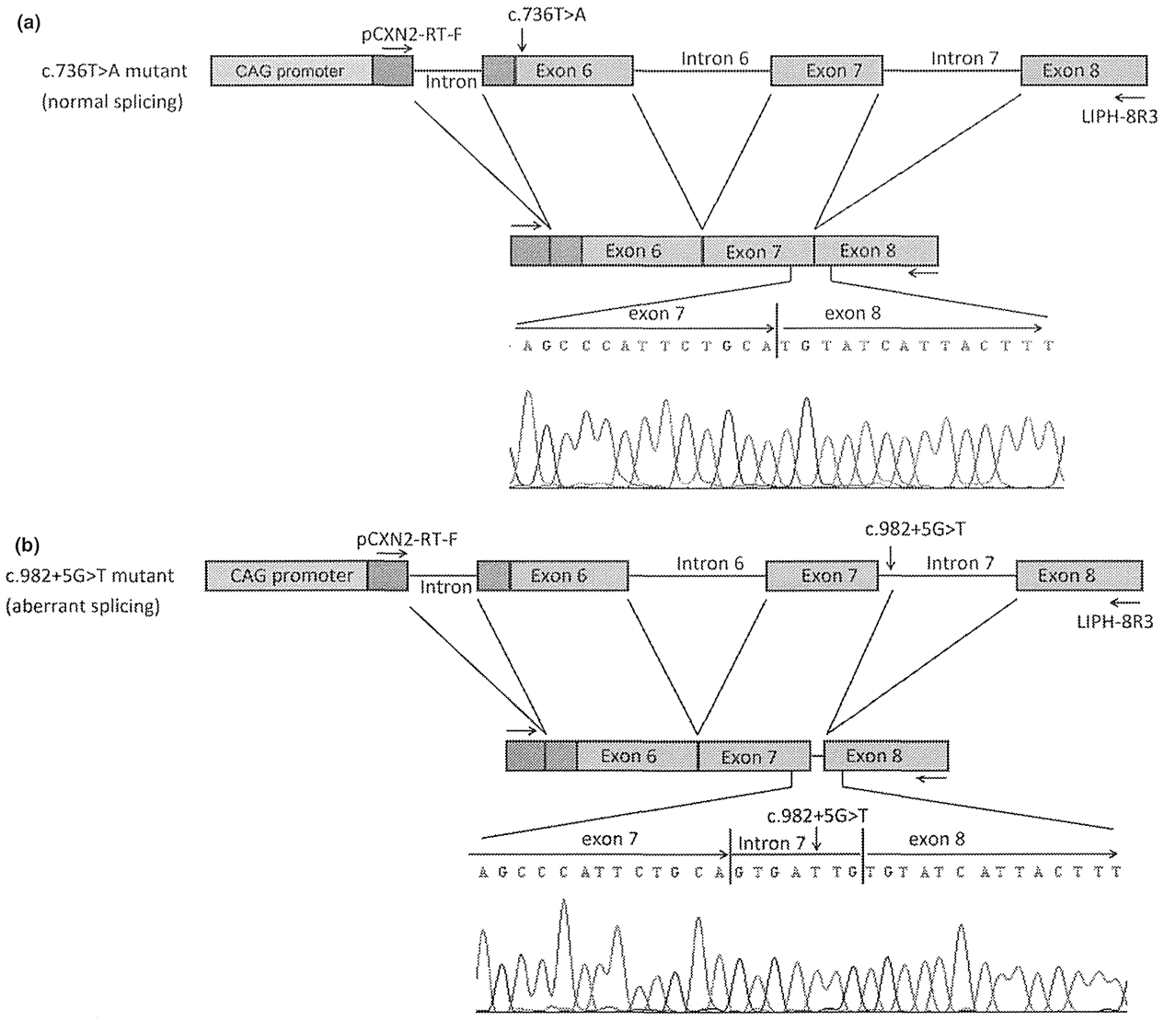

Figure 4. Results of *in vitro* transcription assay. Schematic representation of the mini-gene cassettes of the *LIPH* gene and splicing events from the (a) c.736T>A and the (b) c.982+5G>T mutant constructs are shown. Positions of primers are indicated by arrows. Results of direct sequencing of the polymerase chain reaction product from each mutant allele are also shown. A normal splicing event occurred from the (a) c.736T>A mutant allele, while an aberrant splicing event was induced from the (b) c.982+5G>T mutant allele.

(Invitrogen). Twenty-four hours after the transfection, total RNA was extracted from the cells using the RNeasy Minikit (Qiagen, Valencia, CA, USA). Then, the first-strand cDNA was generated as described above. PCR was performed using a vector-specific forward primer (pCXN2-RT-F: 5′-TCTGACTGACCGCG TTACTC-3′) and an *LIPH*-specific reverse primer (LIPH-8R3). The amplified products were run on 1% agarose gels, and were analyzed by direct sequencing.

RESULTS

Identification of compound heterozygous mutations in the *LIPH* gene

Based on the clinical features, we diagnosed the patient as having ARWH, and searched for mutations in the *LIPH* gene. Direct sequencing analysis revealed that the patient had two distinct heterozygous variants in the *LIPH* gene: a recurrent c.736T>A missense mutation (p.Cys246Ser) in exon 6 and a nucleotide substitution c.982+5G>T in intron 7 of the *LIPH* gene (Fig. 2a). To screen for the c.982+5G>T variant, we investigated 100 ethnically matched control individuals using the *Dra*III restriction enzyme, which did not identify any carrier in the control population, suggesting that the c.982+5G>T variant could be a pathogenic mutation (Fig. 2b; data not shown). We also confirmed that these two mutations were on different alleles (Fig. 2c).

Only the *LIPH*-mRNA from the c.736T>A allele was stably expressed in the patient's blood

In order to investigate the expression of the mutant *LIPH* transcripts in the patient, we performed RT–PCR using patient's blood-derived RNA. Note that we extracted total RNA from the blood sample, as the *LIPH* gene is known to be expressed in blood,[6] and we could not obtain skin biopsy or plucked hairs from the patient. A single fragment corresponding to the size of the *LIPH* cDNA was amplified from all the samples analyzed, the intensity of which was variable, most likely due to difference in the amount of *LIPH* expressing cells between the blood samples used in this experiment (Fig. 3a). Direct sequencing of the RT–PCR product from the patient revealed only the c.736T>A allele, which strongly suggested that the other allele with the mutation c.982+5G>T may cause a splicing error and lead to the generation of a highly unstable transcript (Fig. 3b).

Mutation c.982+5G>T led to an aberrant splicing event *in vitro*

To further investigate the splicing error caused by the mutation c.982+5G>T, we performed *in vitro* transcription assay in HEK293T cells with the c.736T>A and the c.982+5G>T minigene cassettes of the *LIPH* gene spanning the genomic region from exon 5 to exon 8 (Fig. 4). RT–PCR to detect the transcripts from the constructs showed a similarly sized fragment from each mutant allele (data not shown). However, direct sequencing of the RT–PCR products showed a normal splicing event from the c.736T>A mutant allele (Fig. 4a), whereas the mutation c.982+5G>T led to an aberrant splicing event via using two nucleotides downstream of the mutation as an alternate splice donor site (Fig. 4b). The resultant transcript abnormally contained the first 7-nucleotide sequences of intron 7 (Fig. 4b).

DISCUSSION

In this study, we identified a Japanese patient with ARWH and found compound heterozygous mutations in the *LIPH* gene. Of these, the mutation c.736T>A (p.Cys246Ser) was a well-known founder mutation in the Japanese population, while the c.982+5G>T was a novel mutation. As the mutation c.982+5G>T occurred close to the junction between exon 7 and intron 7, we postulated that it could destroy the splice donor site and cause an aberrant splicing event. RT–PCR experiment using the patient's blood did not detect the *LIPH* transcript from the c.982+5G>T allele (Fig. 3). Furthermore, *in vitro* transcription assay demonstrated an alternative splicing event from the c.982+5G>T allele which was predicted to lead to a frame-shift and a premature termination codon (p.Met328Serfs*41) (Fig. 4). Collectively, it is highly likely that the *LIPH* transcript with the mutation c.982+5G>T was largely degraded through nonsense-mediated mRNA decay,[25] even though it is uncertain if the same splicing event happened *in vivo* or not. Perhaps, another aberrant splicing, such as skipping exon 7, might have occurred *in vivo*, which was under detectable level in our experiments. Before our finding, only one splice site mutation in the *LIPH* gene, c.629-1G>C (Ivs4-1G>C), was reported in the published work;[17] thus, the c.982+5G>T is the second splice site mutation identified in the *LIPH* gene.

Including the mutation c.982+5G>T, a total of six pathogenic mutations in the *LIPH* gene have been identified in the Japanese population: five of these were missense mutations, all of which occurred at a critical amino acid residue for the function of mPA-PLA$_1\alpha$ (Fig. 5).[15,16,19,20,22] Regarding the two prevalent *LIPH* mutations, c.736T>A (p.Cys246Ser) and c.742C>A (p.His248Asn), the correlations between the mutations and the severity in hair phenotype have been suggested, namely, p.His248Asn may be associated with a more severe phenotype (hypotrichosis or complete alopecia) as compared to p.Cys246Ser.[23] However, we have experienced some

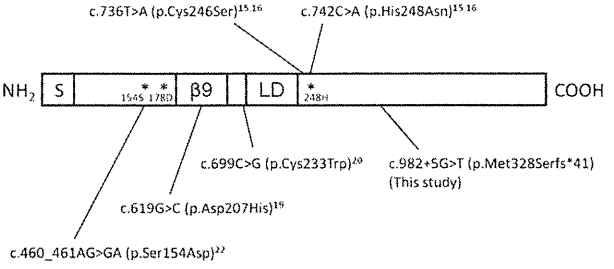

Figure 5. Schematic representation of mPA-PLA$_1\alpha$ protein and position of the *LIPH* mutations identified in the Japanese population. Asterisks indicate the catalytic residues. β9, β9 loop domain; LD, lid domain; S, signal peptide.

exceptions arguing this theory, for example, patients with the homozygous p.His248Asn mutation showed WH with mild hypotrichosis, which was indistinguishable from those with the homozygous p.Cys246Ser mutation (Dr Y. Shimomura, pers. comm., 2014). Therefore, further collection of patients with ARWH and the mutation analysis need to be performed to disclose the genotype–phenotype correlations for the *LIPH* mutations in the Japanese population.

ACKNOWLEDGMENTS: We thank Drs Satoshi Ishii (Akita University, Japan) and Junichi Miyazaki (Osaka University, Japan) for supplying the pCXN2.1 vector. This study was supported in part by a grant from the Takeda Science Foundation, Japan (to Y. S.), and by the "Research on Measures for Intractable Diseases" Project: matching fund subsidy (H26-077) from Ministry of Health, Labor and Welfare, Japan.

CONFLICT OF INTEREST: None declared.

REFERENCES

1 Shimomura Y. Congenital hair loss disorders: rare, but not too rare. *J Dermatol* 2012; **39**: 3–10.
2 Kazantseva A, Goltsov A, Zinchenko R *et al.* Human hair growth deficiency is linked to a genetic defect in the phospholipase gene LIPH. *Science* 2006; **314**: 982–985.
3 Shimomura Y, Wajid M, Petukhova L, Shapiro L, Christiano AM. Mutations in the lipase H gene underlie autosomal recessive woolly hair/hypotrichosis. *J Invest Dermatol* 2009; **129**: 622–628.
4 Pasternack SM, von Kügelgen I, Aboud KA *et al.* G protein-coupled receptor P2Y5 and its ligand LPA are involved in maintenance of human hair growth. *Nat Genet* 2008; **40**: 329–334.
5 Shimomura Y, Wajid M, Ishii Y *et al.* Disruption of P2RY5, an orphan G protein-coupled receptor, underlies autosomal recessive woolly hair. *Nat Genet* 2008; **40**: 335–339.
6 Sonoda H, Aoki J, Hiramatsu T *et al.* A novel phosphatidic acid-selective phospholipase A1 that produces lysophosphatidic acid. *J Biol Chem* 2002; **277**: 34254–34263.
7 Yanagida K, Masago K, Nakanishi H *et al.* Identification and characterization of a novel lysophosphatidic acid receptor, p2y5/LPA6. *J Biol Chem* 2009; **284**: 17731–17741.
8 Inoue A, Arima N, Ishiguro J, Prestwich GD, Arai H, Aoki J. LPA-producing enzyme PA-PLA$_1\alpha$ regulates hair follicle development by modulating EGFR signaling. *EMBO J* 2011; **30**: 4248–4260.
9 Fujimoto A, Farooq M, Fujikawa H *et al.* A missense mutation within the helix initiation motif of the keratin K71 gene underlies autosomal dominant woolly hair/hypotrichosis. *J Invest Dermatol* 2012; **132**: 2342–2349.
10 Ali G, Chishti MS, Raza SI, John P, Ahmad W. A mutation in the lipase H (LIPH) gene underlie autosomal recessive hypotrichosis. *Hum Genet* 2007; **121**: 319–325.
11 Nahum S, Pasternack SM, Pforr J *et al.* A large duplication in LIPH underlies autosomal recessive hypotrichosis simplex in four Middle Eastern families. *Arch Dermatol Res* 2009; **301**: 391–393.
12 Shimomura Y, Wajid M, Zlotogorski A, Lee YJ, Rice RH, Christiano AM. Founder mutations in the lipase h gene in families with autosomal recessive woolly hair/hypotrichosis. *J Invest Dermatol* 2009; **129**: 1927–1934.
13 Pasternack SM, von Kügelgen I, Müller M *et al.* In vitro analysis of LIPH mutations causing hypotrichosis simplex: evidence confirming the role of lipase H and lysophosphatidic acid in hair growth. *J Invest Dermatol* 2009; **129**: 2772–2776.
14 Naz G, Khan B, Ali G *et al.* Novel missense mutations in lipase H (LIPH) gene causing autosomal recessive hypotrichosis (LAH2). *J Dermatol Sci* 2009; **54**: 12–16.
15 Shimomura Y, Ito M, Christiano AM. Mutations in the LIPH gene in three Japanese families with autosomal recessive woolly hair/hypotrichosis. *J Dermatol Sci* 2009; **56**: 205–207.
16 Shinkuma S, Akiyama M, Inoue A *et al.* Prevalent LIPH founder mutations lead to loss of P2Y5 activation ability of PA-PLA1alpha in autosomal recessive hypotrichosis. *Hum Mutat* 2010; **31**: 602–610.
17 Kalsoom UE, Habib R, Khan B *et al.* Mutations in lipase H gene underlie autosomal recessive hypotrichosis in five Pakistani families. *Acta Derm Venereol* 2010; **90**: 93–94.
18 Tariq M, Azhar A, Baig SM, Dahl N, Klar J. A novel mutation in the Lipase H gene underlies autosomal recessive hypotrichosis and woolly hair. *Sci Rep* 2012; **2**: 730.
19 Shinkuma S, Inoue A, Aoki J *et al.* The β9 loop domain of PA-PLA1α has a crucial role in autosomal recessive woolly hair/hypotrichosis. *J Invest Dermatol* 2012; **132**: 2093–2095.
20 Yoshizawa M, Nakamura M, Farooq M, Inoue A, Aoki J, Shimomura Y. A novel mutation, c.699C>G (p. C233W), in the LIPH gene leads to a loss of the hydrolytic activity and the LPA6 activation ability of PA-PLA1α in autosomal recessive wooly hair/hypotrichosis. *J Dermatol Sci* 2013; **72**: 61–64.
21 Mehmood S, Jan A, Muhammad D *et al.* Mutations in the lipase-H gene causing autosomal recessive hypotrichosis and woolly hair. *Australas J Dermatol* 2014; Mar 13. doi: 10.1111/ajd.12157. [Epub ahead of print].
22 Hayashi R, Akasaka T, Ito M, Shimomura Y. Compound heterozygous mutations in two distinct catalytic residues of the LIPH gene underlie autosomal recessive woolly hair in a Japanese family. *J Dermatol* 2014; (in press).
23 Tanahashi K, Sugiura K, Kono M *et al.* Highly prevalent LIPH founder mutations causing autosomal recessive woolly hair/hypotrichosis in Japan and the genotype/phenotype correlations. *PLoS One* 2014; **9**: e89261.
24 Niwa H, Yamamura K, Miyazaki J. Efficient selection for high-expression transfectants with a novel eukaryotic vector. *Gene* 1991; **108**: 193–199.
25 Frischmeyer PA, Dietz HC. Nonsense-mediated mRNA decay in health and disease. *Hum Mol Genet* 1999; **8**: 1893–1900.

Acta Derm Venereol 2014; 94: 337–339

SHORT COMMUNICATION

Immunosuppressive and Cytotoxic Cells in Invasive versus Non-invasive Bowen's Disease

Sadanori Furudate, Taku Fujimura*, Yumi Kambayashi, Takahiro Haga, Akira Hashimoto and Setsuya Aiba

*Department of Dermatology, Tohoku University Graduate School of Medicine, Seiryo-machi 1-1, Aoba-ku, Sendai 980-8574, Japan. *E-mail: tfujimura1@mac.com*

Accepted Aug 6, 2013; Epub ahead of print Oct 24, 2013

Bowen's disease (BD) is defined as epidermal carcinoma *in situ* that may progress to invasive BD retaining the cytological characteristics of BD (1). Previous reports suggested the contribution of tumour infiltrating leukocytes around the tumour, including regulatory T cells (Tregs), in organising the tumour microenvironment (2). In this report, we hypothesised that the profiles of tumour-infiltrating leukocytes might be correlated with the invasion of BD.

MATERIALS AND METHODS

We collected archival formalin-fixed paraffin-embedded skin specimens from 5 patients with BD, 5 patients with micro-invasive BD and patients with invasive BD treated in the Department of Dermatology at Tohoku University Graduate School of Medicine (Table SI[1]). All diagnoses were made by typical clinical manifestations and histopathological examination. Two dermatologists counted and estimated by blind assessment the infiltrated lymphocytes. Antibodies (Abs) for immunohistochemical staining were then used, as described previously (3) (Table SII[1]).

RESULTS

We performed immunohistochemical staining of CD163 (Fig. 1) as well as Foxp3 (Fig. S1[1]). Only in invasive BD, dense CD163$^+$ MΦ were detected throughout the dermis. In contrast to CD163$^+$ cells, the number of Foxp3$^+$ cells was significantly lower in invasive BD (Fig. 2).

Next, in order to compare the profiles of tumour-infiltrating CTLs between invasive, micro-invasive and non-invasive BD, we employed immunohistochemical staining for CD8 (Fig. S2A–C[1]), granulysin (Fig. S2D–F) and TIA-1 (Fig. S2 G, I[1]). There was no significant difference in the numbers of CD8$^+$ cells, granulysin$^+$ cells and TIA-1$^+$ cells among these groups (see Fig. 2).

To further investigate the immunosuppression in the tumour microenvironment, we employed immunohistochemical staining for B7H1 (ProSci, Poway, CA) and MMP9. Interestingly, in non-invasive BD, B7H1 was strongly expressed on tumour cells (Fig. 3A). In contrast, B7H1 expressing cells were mainly observed on the tumour-infiltrating leukocytes around the tumour in micro-invasive (Fig. 3B) and invasive BD (Fig. 3C). Dense infiltration of MMP9$^+$ cells was detected around the tumour in invasive BD (Fig. 3D), while few MMP9$^+$ cells were detected around the tumour in non-invasive BD (Fig. 3E) and micro-invasive BD (Fig. 3F).

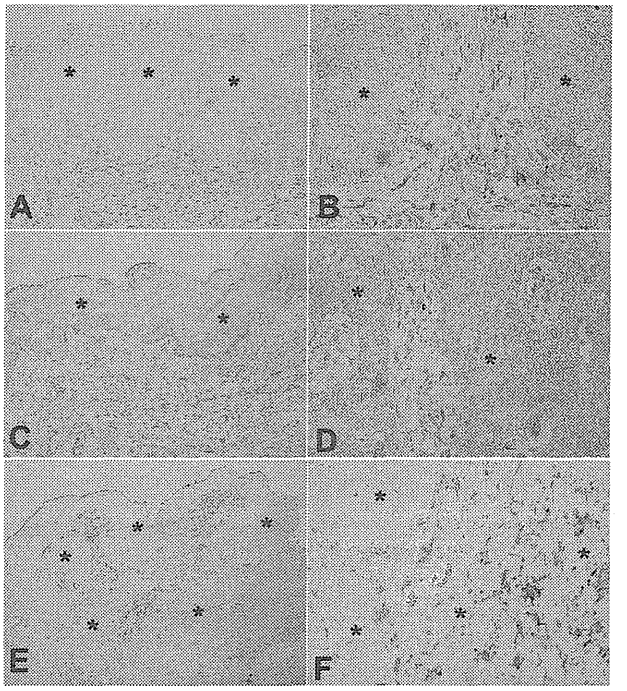

Fig. 1. CD163$^+$ M2 MΦ in non-invasive, micro-invasive and invasive Bowen's disease (BD). Paraffin-embedded tissue samples from patients with non-invasive BD (A, B), micro-invasive BD (C, D) and invasive BD (E, F) were deparaffinised and stained with anti-CD163 Ab (A–F). Sections were developed with liquid permanent red. (CD163: staining for MΦ) (A, C, E: ×100; B, D, F: ×400). (Asterisk: Tumour site).

DISCUSSION

Our results demonstrated dense infiltration of CD163$^+$ MΦ throughout the dermis only in invasive BD. Recent reports suggested that the presence of macrophages correlates with therapy failure and poor prognosis in cancer patients (4, 5). More recently, it was reported that M2 MΦ cells have an important role in the production of thymus and activation-regulated chemokine, which leads to the induction of Tregs and Th2, and the composition of the immunosuppressive tumour microenvironment (6, 7). Therefore we hypothesised that there is correlation between the increasing numbers of M2MΦ and the numbers of Tregs. Unexpectedly, in contrast to the increasing

[1]http://www.medicaljournals.se/acta/content/?doi=10.2340/00015555-1729

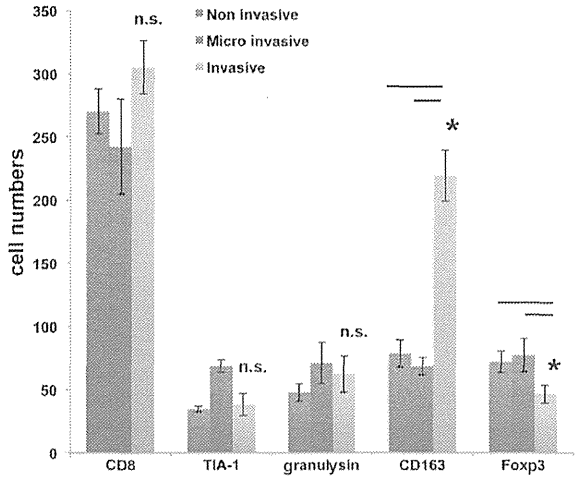

Fig. 2. Summary of the numbers of $CD8^+$ cells, TIA-1^+ cells, granulysin bearing cells, $CD163^+$ cells and $Foxp3^+$ cells in non-invasive, micro-invasive and invasive Bowen's disease. Five representative fields of each section were selected from both the epidermis and the dermis associated with dense dermal lymphoid infiltrate. The number of immunoreactive cells was counted using an ocular grid of 1 cm^2 at a magnification of ×400. The data are expressed as the mean ± SD of the numbers in each area. $*p<0.05$.

number of M2MΦ, the number of Tregs is significantly decreased in invasive BD. This discrepancy might be explained by the expression of B7H1 in tumour and M2MΦ cells. Indeed, in our study, the high expression of B7H1 in tumour cells is only prominent in non-invasive BD, which might be connected with the increased numbers of Tregs (8). Instead of B7H1 expression in tumour cells, invasive BD contains B7H1-expressing cells and MMP9-expressing cells around the tumour. As previously suggested, the expression of MMP9 in immunosuppressive macrophages in the tumour microenvironment contributed to tumour invasion and metastasis (3, 9, 10).

To further investigate the immunological environment of BD, we investigated the population of cytotoxic T cells, focusing on CD8, granulysin and TIA-1. CD8 is a classical common marker for cytotoxic T cells, while granulysin and TIA-1 have been reported to be functional markers for cytotoxic T cells, and correlate with the prognosis of cancer patients (11–13). In contrast to immunosuppressive cells, there was no significant difference in tumour infiltrating cytotoxic T cells at any stage of BD, suggesting that the immunological background of the tumour microenvironment in BD might be determined by immunosuppressive cells such as M2 MΦ and Tregs. Since we did not directly assess the suppressive function of these infiltrating M2 MΦ or cytotoxic T cells, further analysis of the mechanisms underlying this phenomenon will be necessary to confirm our limited observation.

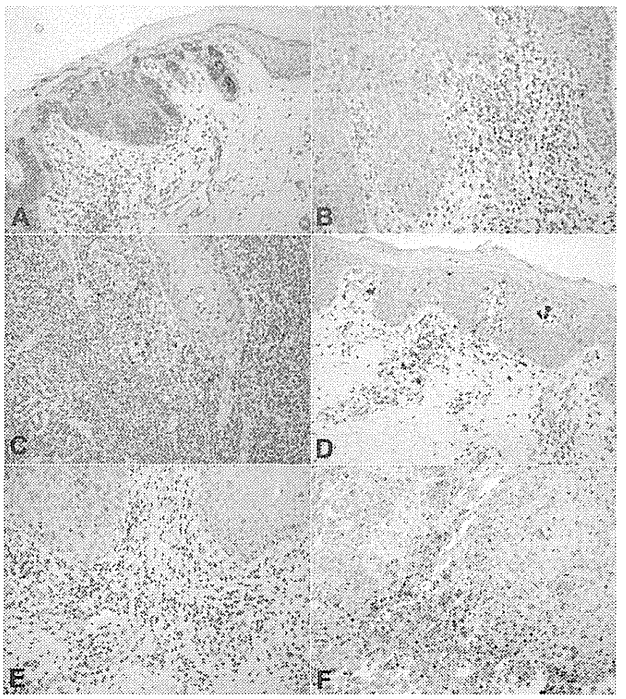

Fig. 3. The expression of B7H1 and MMP9 in non-invasive, micro-invasive and invasive Bowen's disease. Paraffin-embedded tissue samples from patients with non-invasive BD (A, D), micro-invasive BD (B, E) and invasive BD (C, F) were deparaffinised and stained with anti-B7H1 Ab (A–C) or with anti-MMP9 AB (D–F). Sections were developed with liquid permanent red. (A–F: original manifestation ×200).

REFERENCES

1. Mii S, Amoh Y, Tanabe K, Kitasato H, Sato Y, Katsuoka K. Nestin expression in Bowen's disease and Bowen's carcinoma associated with human papillomavirus. Eur J Dermatol 2011; 21: 515–519.
2. Liao WT, Yu CL, Lan CC, Lee CH, Chang CH, Chang LW, et al. Differential effects of arsenic on cutaneous and systemic immunity: focusing on CD4+ cell apoptosis in patients with arsenic-induced Bowen's disease. Carcinogenesis 2009; 30: 1064–1072.
3. Kambayashi Y, Fujimura T, Aiba S. Comparison of immunosuppressive and immunomodulatory cells in keratoacanthoma and cutaneous squamous cell carcinoma. Acta Derm Venereol 2013; 93: 663–668.
4. Steidl C, Lee T, Shah SP, Farinha P, Han G, Nayar T, et al. Tumor-associated macrophages and survival in classic Hodgkin's lymphoma. N Engl J Med 2010; 362: 875–885.
5. Zhu XD, Zhang JB, Zhuang PY, Zhu HG, Zhang W, Xiong YQ, et al. High expression of macrophage colony-stimulating factor in peritumoral liver tissue is associated with poor survival after curative resection of hepatocellular carcinoma. J Clin Oncol 2008; 26: 2707–2716.
6. Satoh T, Takeuchi O, Vandenbon A, Yasuda K, Tanaka Y, Kumagai Y, et al. The Jmjd3-Irf4 axis regulates M2 macrophage polarization and host responses against helminth infection. Nat Immunol 2010; 11: 936–944.
7. Jones K, Vari F, Keane C, Crooks P, Nourse JP, Seymour LA, et al. Serum CD163 and TARC as disease response biomarkers in classical Hodgkin lymphoma. Clin Cancer Res 2013; 19: 731–742.
8. Fujimura T, Ring S, Umansky V, Mahnke K, Enk AH. Regulatory T cells (Treg) stimulate B7-H1 expression in myeloid derived suppressor cells (MDSC) in ret melanomas. J Invest Dermatol 2012; 132: 1239–1246.
9. Kambayashi Y, Fujimura T, Furudate S, Hashimoto A, Haga T, Aiba S. Comparison of immunosuppressive cells

and cytotoxic cells in angiosarcoma: the development of a possible supportive therapy for angiosarcoma. Dermatology 2013; 227: 14–20.
10. Melani C, Sangaletti S, Barazzetta FM, Werb Z, Colombo MP. Amino-biphosphonate-mediated MMP-9 inhibition breaks the tumor-bone marrow axis responsible for myeloid derived suppressor cell expansion and macrophage infiltration in tumor stroma. Cancer Res 2007; 67:11438–11446.
11. Kitamura N, Katagiri YU, Itagaki M, Miyagawa Y, Onda K, Okita H, et al. The expression of granulysin in systemic anaplastic large cell lymphoma in childhood. Leuk Res 2009; 33: 908–912.
12. Alvaro T, Lejeune M, Salvadó MT, Bosch R, García JF, Jaén J, et al. Outcome in Hodgkin's lymphoma can be predicted from the presence of accompanying cytotoxic and regulatory T cells. Clin Cancer Res 2005; 11: 1467–1473.
13. Fujimura T, Furudate S, Kambayashi Y, Aiba S. Potential use of bisphosphonates in invasive extramammary Paget's disease: an immunohistochemical Investigation. Clin Dev Immunol 2013: 164982.

Acta Derm Venereol 2014; 94: 104–106

SHORT COMMUNICATION

Induction of CD163$^+$ M2 Macrophages in the Lesional Skin of Eosinophilic Pustular Folliculitis

Akiko Hagiwara, Taku Fujimura, Sadanori Furudate, Yumi Kambayashi, Saori Kagatani and Setsuya Aiba
Department of Dermatology, Tohoku University Graduate School of Medicine, Seiryo-machi 1-1, Aoba-ku, Sendai, 980-8574, Japan. E-mail: tfujimura1@mac.com
Accepted Feb 4, 2013; Epub ahead of print Apr 19, 2013

Eosinophilic pustular folliculitis (EPF) is a rare dermatitis of unknown aetiology, characterized by recurrent clusters of pruritic, follicular, sterile papules and pustules on the face, trunk and upper extremities (1). EPF is often accompanied by peripheral blood eosinophilia, and a T-helper (Th) 2 cytokine-dominant condition has been postulated as a possible underlying mechanism (2). Macrophages are functionally polarized into M1 and M2 cells; M2 macrophages have important roles in the response to parasite infection, tissue remodelling, angiogenesis and tumour-progression, and have been shown to be involved in Th2 polarization (3). STAT6 participates in Th2 differentiation by enhancing expression of the master regulator of Th2 differentiation, GATA3 (4). STAT6 and GATA3, together with interleukin (IL)-2-mediated STAT5 activation, induce the secretion of copious amounts of IL-4, IL-5 and IL-13 by activated Th2 cells (5). In the present case, we investigated the immunohistochemical profiles of perifollicular and interstitial infiltrating cells, focusing on the profiles of immunosuppressive cells and Th2 signals.

CASE REPORT

A 64-year-old Japanese man visited our outpatient clinic with a 1-year history of pruritic eruption on his face, trunk and extremities. He had been treated with topical steroids and anti-histamine for 9 months, with no improvement. On his initial visit, physical examination revealed pruritic, indurated, erythematous plaque, with papules and pustules on the face (Fig. 1A). In addition, there were groups of firm, waxy red papules, 3–4 mm in diameter, on his trunk and extremities (Fig. 1B, C). A full blood count and biochemical profile revealed eosinophilia (13%) (normal < 10%) and increased IgE level (2,130 IU/ml) (normal < 170 IU/ml), although the specific IgEs for MAST 33 allergen were all negative. The serum CCL17/thymus and activation-regulated chemokine (TARC) level was 11,390 pg/ml (normal < 449 pg/ml). Serum HIV antibody was negative. A biopsy specimen from the right cheek revealed exocytosis of eosinophils into a spongiotic follicular infundibulum and the accompanying sebaceous gland (Fig. 2A). Immunohistochemical staining for CD163 (Novocastra, Newcastle upon Tyne, UK), pSTAT6 (Cell Signaling Technology, Tokyo, Japan), and IL-10 (Life Span Bioscience, Seattle, WA, USA) revealed a dense infiltration of CD163$^+$ M2 macrophages (Fig. 2B), pSTAT6$^+$ cells (Fig. 2C) in the dermis and IL-10 producing cells in the perifollicular area (Fig. 2D) (Table SI[1]). The patient was treated with oral prednisolone, 30 mg/day, and levocetirizine hydrochloride, 5 mg/day. The pruritus improved initially, although there was no change in the eruption. However, when oral prednisolone was gradually decreased, the pruritus recurred. Administration of oral prednisolone, 30 mg/day, with narrow-band ultraviolet B (UVB) irradiation, was started, with no improvement. Subsequently, the patient was started on oral cyclosporine, 3 mg/kg/day, with oral prednisolone, 15 mg/day. His pruritus and eruption improved during one week, in parallel with a decrease in the serum TARC level (220 pg/ml). There was no sign of relapsing pruritic papules.

DISCUSSION

In this case report, we employed immunohistochemical staining for CD163, which is known as a marker for alternative activated M2 macrophages (6, 7), in a case of classic, non-immunosuppression-associated EPF. Interestingly, CD163$^+$ M2 macrophages densely infiltrated the

[1]http://www.medicaljournals.se/acta/content/?doi=10.2340/00015555-1612

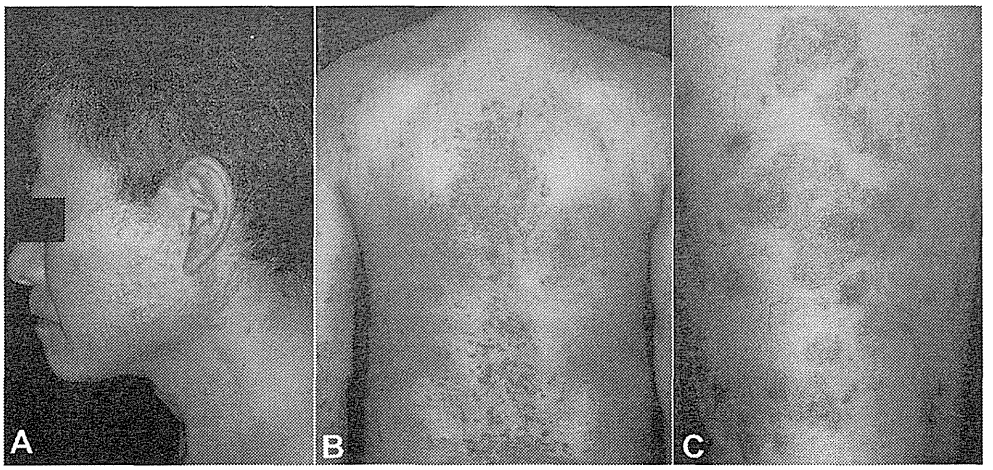

Fig. 1. (A) A pruritic, indurated, erythematous plaque with papules and pustules on the face. Groups of firm, waxy red papules, 3–4 mm in diameter on (B) the trunk and (C) extremities. Permission to publish this photo is given from the patient.

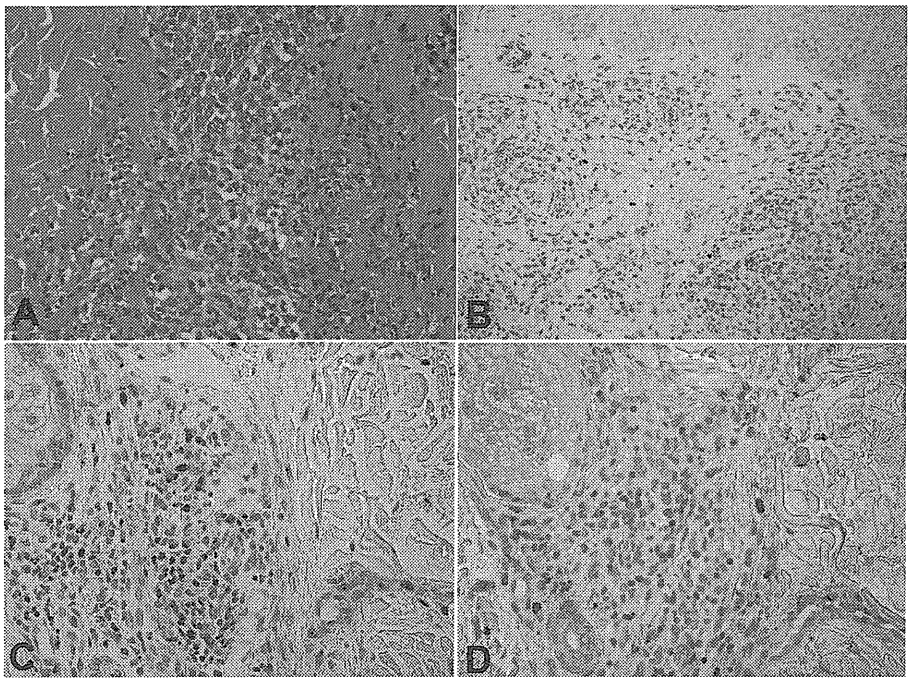

Fig. 2. (A) Exocytosis of eosinophils into a spongiotic follicular infundibulum and accompanying sebaceous gland. The paraffin-embedded tissue sample was deparaffinized and stained using (B) anti-CD163 Ab, (C) anti-pSTAT6 Ab, or (D) anti IL-10 Ab. The sections were developed with liquid permanent red for CD163 and IL-10, (*red*) and with 3,3'-diaminobenzidine tetrahydrochloride for pSTAT6 (*brown*) (original magnification: A, C, D ×400; B ×200).

interstitial area of the dermis and perifollicular areas of the lesional skin. In addition, the expression of pSTAT6 on infiltrating cells, IL-10 producing cells in the dermis and the high levels of serum TARC suggested the contribution of Th2 cells to the establishment of EPF. Our case might suggest possible mechanisms of development of EPF through CD163 M2 macrophages and Th2 pathways.

Alternatively activated macrophages, M2 macrophages, have an important role in the response to parasite infection, tissue remodelling, angiogenesis and tumour-progression (3). Satoh et al. (3) reported that Jumonji domain-containing-3 (Jmjd3) is essential for M2 macrophage polarization and targeting transcription factor interferon-regulatory factor 4 (Irf4), which has been shown to be involved in Th2 polarization. Interestingly, Otsuka et al. (2) reported the upregulation of Th2 cytokine-related mRNA in peripheral blood mononuclear cells from patients with EPF who were successfully treated with cyclosporine. This report suggests the contribution of Th2 cytokines to the pathogenesis of EPF. In humans, CD163, the scavenger receptor cysteine-rich family type B, is reported to be a marker for M2 macrophages in dermatological fields (6, 7). In our present study, $CD163^+$ M2 macrophages were predominantly infiltrated in the interstitial area of the dermis, which might suggest the contribution of M2 macrophages to EPF. In addition, to confirm the contribution of $CD163^+$ M2 macrophages to EPF, we employed immunohistochemical staining in a CD163 for an additional 4 cases of classic EPF, and in all cases substantial numbers of $CD163^+$ cells were detected (data not shown).

STATs are latent transcription factors that reside in the cytoplasm until activated. Phosphorylated STAT enters the nucleus and binds specific regulatory sequences to activate or repress the transcription of target genes (8). STAT1 is activated by Th1 cytokines such as IFN-α/β, IFN-γ and IL-27 (9), whereas STAT6 is activated by IL-4 (10). STAT6 participates in Th2 differentiation by enhancing the expression of the master regulator of Th2 differentiation, GATA3 (10). STAT6 and GATA3, together with IL-2-mediated STAT5 activation, induce the secretion of copious amounts of IL-4, IL-5 and IL-13 by activated Th2 cells (11).

Non-steroidal anti-inflammatory drugs (NSAIDs), including indomethacin, are used clinically for the treatment of EPF, although the precise mechanisms for the effect of NSAIDs on EPF are still under discussion (12). Interestingly, bioactive lipids, such as prostaglandin E2, are known to be major contributors to amplifying the arginase 1 level, which is known as a suppressive marker for suppressive macrophages, such as M2 macrophages and myeloid-derived suppressor cells (13, 14). In our present case, we initially administered oral steroid with no improvement. The additional administration of cyclosporine dramatically improved the eruption. A previous report also suggested that glucocorticoids generate M2 macrophages (15). The present case suggests a possible therapy for EPF by targeting M2 macrophages/ Th2 cytokine pathways.

REFERENCES

1. Ofuji S, Ogino A, Horio T, Oseko T, Uehara M. Eosinophilic pustular folliculitis. Acta Derm Venereol 1970; 50: 195–203.
2. Otsuka A, Doi H, Miyachi Y, Kabashima K. Treatment of eosinophilic pustular folliculitis with ciclosporin: suppres-

sion of mRNA expression of IL-4 and IL-13. J Eur Acad Dermatol Venereol 2010; 24: 1489–1491.
3. Satoh T, Takeuchi O, Vandenbon A, Yasuda K, Tanaka Y, Kumagai Y, et al. The Jmjd3-Irf4 axis regulates M2 macrophage polarization and host responses against helminth infection. Nat Immunol 2010; 11: 936–944.
4. Chapoval S, Dasgupta P, Dorsey NJ, Keegan AD. Regulation of the T helper cell type 2 (Th2)/T regulatory cell (Treg) balance by IL-4 and STAT6. J Leukoc Biol 2010; 87: 1011–1018.
5. Zhu J, Jankovic D, Grinberg A, Guo L, Paul WE. Gfi-1 plays an important role in IL-2-mediated Th2 cell expansion. Proc Natl Acad Sci U S A 2006; 103: 18214–18219.
6. Fuentes-Duculan J, Suárez-Fariñas M, Zaba LC, Nograles KE, Pierson KC, Mitsui H, et al. A subpopulation of CD163-positive macrophages is classically activated in psoriasis. J Invest Dermatol 2010; 130: 2412–2422.
7. Fujimura T, Kambayashi Y, Hidaka T, Hashimoto A, Haga T, Aiba S. Comparison of Foxp3+ regulatory T-cells and CD163+ macrophages in invasive and non-invesive extramammary Paget's disease. Acta Derm Venereol 2012, 92: 625–628.
8. Adamson AS, Collins K, Laurence A, O'Shea JJ. The Current STATus of lymphocyte signaling: new roles for old players. Curr Opin Immunol 2009; 21: 161–166.
9. Kotenko SV, Gallagher G, Baurin VV, Lewis-Antes A, Shen M, Shah NK, et al. IFN-lambdas mediate antiviral protection through a distinct class II cytokine receptor complex. Nat Immunol 2003; 4: 69–77.
10. Chapoval S, Dasgupta P, Dorsey NJ, Keegan AD. Regulation of the T helper cell type 2 (Th2)/T regulatory cell (Treg) balance by IL-4 and STAT6. J Leukoc Biol 2010; 87: 1011–1018.
11. Zhu J, Jankovic D, Grinberg A, Guo L, Paul WE. Gfi-1 plays an important role in IL-2-mediated Th2 cell expansion. Proc Natl Acad Sci U S A 2006; 103: 18214–18219.
12. Katoh M, Nomura T, Miyachi Y, Kabashima K. Eosinophilic pustular folliculitis: A review of the Japanese published works. J Dermatol 2013; 40: 15–20.
13. Rodriguez PC, Hernandez CP, Quiceno D, Dubinett SM, Zabaleta J, Ochoa JB, et al. Arginase 1 in myeloid suppressor cells is induced by COX-2 in lung carcinoma. J Exp Med 2005; 202: 931.
14. Fujimura T, Mahnke K, Enk AH. Myeloid derived suppressor cells and their role in tolerance induction in cancer. J Dermatol Sci 2010; 59: 1–6.
15. Gordon S. Alternative activation of macrophages. Nat Rev Immunol 2003; 3: 23–35.

Acta Derm Venereol 2014; 94: 223–224

SHORT COMMUNICATION

Generalized Granulomatous Dermatitis Accompanied by Myelodysplastic Syndrome

Akiko Hagiwara, Taku Fujimura, Sadanori Furudate, Yumi Kambayashi, Yukikazu Numata, Takahiro Haga and Setsuya Aiba
Department of Dermatology, Tohoku University Graduate School of Medicine, Seiryo-machi 1-1, Aoba-ku, Sendai, 980-8574, Japan.
E-mail: tfujimura1@mac.com
Accepted Apr 4, 2013; Epub ahead of print Jul 1, 2013

Cutaneous manifestations associated with myelodysplastic syndrome (MDS) are uncommon. Recognizing MDS skin manifestations is important as they can precede blood or bone marrow transformation to leukaemia and are associated with a poor prognosis (1, 2). Recently, 2 cases of granulomatous dermatitis associated with MDS were reported as non-specific cutaneous manifestations of MDS, with subsequent development into acute myeloid leukaemia with leukaemia cutis (1, 2). An imbalance of T-cell subsets, regulatory T cells (Tregs) and Th17 in MDS is also correlated with disease progression (3, 4). We describe here a case of granulomatous dermatitis accompanied by MDS, which we hypothesized might show correlations with Tregs and interleukin (IL)-17 producing cells. We therefore employed immunohistochemical staining for Foxp3 and IL-17 to characterize the granuloma.

CASE REPORT

A 65-year-old Japanese man with a one-year history of pruritic eruption on his face, trunk and extremities visited our outpatient clinic. He had been treated with topical steroids and anti-histamine for one year with no improvement. On his initial visit, physical examination revealed erythroderma overlapping with groups of firm nodules on the trunk and extremities (Fig. 1). A biopsy specimen from his right lower leg revealed interstitial, dermal granulomatous inflammation with multinucleated giant cells without blasts, neutrophils or atypical cells (Fig. 2A, B). Eosinophils were not prominent. Immunohistochemical staining revealed that these infiltrating cells were mainly positive for CD3, CD4, CD5, CD7 and CD8, and negative for neutrophil elastase, myeloperoxidase (MPO), Alcian blue and Ziehl-Neelsen stain. The Ki67 score was approximately 10%. Immunohistochemical staining for Foxp3, IL-17 and CD163 revealed dense, massive infiltration of $Foxp3^+$ Tregs throughout the granuloma tissue (Fig. 2C, D), which were surrounded by $CD163^+$ M2 macrophages (Fig. 2E). IL-17-producing cells were scattered in the granuloma tissue (Fig. 2F). A full blood count revealed prominent upregulation of monocytes (45%, 2,750/mm^3). Bone marrow biopsies revealed increased numbers of megakaryocyte (313/μl) and a high ratio of myeloblasts (15.4%). The karyotype of this patient is 46, XY, and the chromosome aberration test revealed 2 types of abnormalities in chromosome (46, XY, der (1) (qter-q21::p32-qter), and 46, XY, t(3; 16) (q27;p11.2)). From the above findings, we diagnosed this patient with generalized granulomatous dermatitis accompanied by myelodysplastic syndrome (Refractory Anemia with Excess of Blasts, type 2 (RAEB2), International Prognostic Scoring System (IPSS) score 2.0) (5). We administered oral prednisolone 30 mg/day, nicotinic acid amide 1.5 mg/day and doxycycline hydrochloride 200 mg/day. His pruritus and eruption improved, although there was no change in the firm nodules on the trunk and extremities.

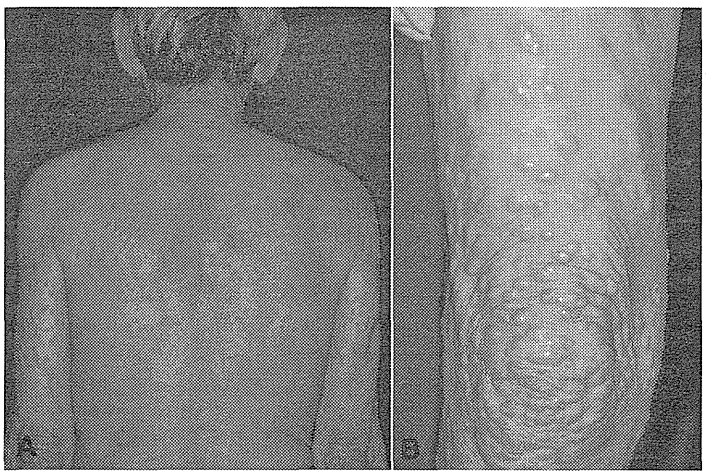

Fig. 1. Erythroderma overlapping with groups of firm nodules on (A) the trunk and (B) extremities.

DISCUSSION

Cutaneous manifestations of myelodysplastic syndrome (MDS) are uncommon and can occur as specific neoplastic infiltrations of malignant hematopoietic cells or various non-specific lesions (3, 4, 6, 7). Among them, granulomatous dermatitis has rarely been reported as a manifestation of MDS (1, 2). Recently, Balin et al. (1) reported a case of granulomatous dermatitis accompanied by MDS, and concluded that granulomatous dermatitis might be the first sign of underlying MDS.

The contribution of an imbalance in T-cell subsets, regulatory T cells (Tregs) and Th17, to MDS has been reported previously (3, 4, 6, 7). In fact, Kordasti et al. (3) reported a significant correlation between increased numbers of $CD4^+$ Tregs and MDS subgroups with disease progression. Moreover, they reported in another study that the Th17:Treg ratio was significantly higher in low-risk MDS compared with high-risk MDS (4). Overall, the prognosis of MDS is strongly correlated with Tregs and Th17. On the other hand, we recently reported the distribution of $Foxp3^+$ Tregs and IL-17-producing cells in several cases of cutaneous granulomatous

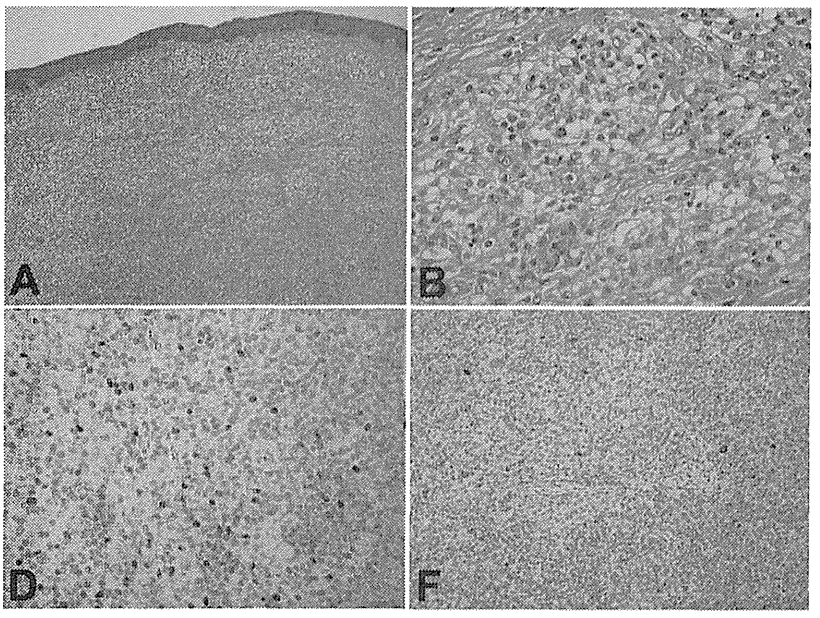

Fig. 2. (A, B) Interstitial, dermal granulomatous inflammation with multinucleated giant cells. The paraffin-embedded tissue sample was deparaffinized and stained using (D) anti-Foxp3 Ab or (F) anti IL-17 Ab. The sections were developed with liquid permanent red. The central area of granuloma is positive for Foxp3$^+$ and negative for CD163$^+$ macrophages. Peripheral areas of granuloma positive for CD163$^+$ macrophages and negative for Foxp3$^+$ Tregs. (Original magnification (A) × 50, (F) × 200, (B) × 400). (Complete figure available from http://www.medicaljournals.se/acta/content/?doi=10.2340/00015555-1656).

dermatitis, including sarcoidosis, granuloma annulare, necrobiosis lipoidica, granulomatous pigmented and purpuric dermatitis (8–10). Therefore, since we hypothesized that our present case, granulomatous dermatitis accompanied by MDS, might show correlations with Tregs and IL-17-producing cells, we employed immunohistochemical staining for Foxp3 and IL-17 to characterize the granuloma. As we expected, based on previous reports (3, 4, 6–10), Foxp3$^+$ Tregs were predominant in the granuloma cells, similar to sarcoidosis, whereas IL-17-producing cells were scattered. In addition, CD163$^+$ M2 macrophages, which are also known to correlate with Th2 and Tregs (11, 12), were detected around the granuloma. Like suppressive macrophages, myeloid-derived suppressor cells in tumour-bearing host (13), these CD163$^+$ M2 macrophages might be related to the induction of Tregs in granuloma. Since we did not directly assess the suppressive function of these infiltrating Tregs and M2 macrophages, further research into the mechanisms underlying this phenomenon may provide fundamental insights into the mechanisms of granulomatous dermatitis with MDS.

REFERENCES

1. Balin SJ, Wetter DA, Kurtin PJ, Letendre L, Pittelkow MR. Myelodysplastic syndrome presenting as generalized granulomatous dermatitis. Arch Dermatol 2011; 147: 331–335.
2. Cornejo KM, Lum CA, Izumi AK. A cutaneous interstitial granulomatous dermatitis-like eruption arising in myelodysplasia with leukemic progression. Am J Dermatopathol 2013; 35: e26–29.
3. Kordasti SY, Ingram W, Hayden J, Darling D, Barber L, Afzali B, et al. CD4+CD25high Foxp3+ regulatory T cells in myelodysplastic syndrome (MDS). Blood 2007; 110: 847–850.
4. Kordasti SY, Afzali B, Lim Z, Ingram W, Hayden J, Barber L, et al. IL-17-producing CD4(+) T cells, pro-inflammatory cytokines and apoptosis are increased in low risk myelodysplastic syndrome. Br J Haematol 2009; 145: 64–72.
5. Alessandrino EP, Della Porta MG, Bacigalupo A, Van Lint MT, Falda M, Onida F, et al. WHO classification and WPSS predict posttransplantation outcome in patients with myelodysplastic syndrome: a study from the Gruppo Italiano Trapianto di Midollo Osseo (GITMO). Blood 2008; 112: 895–902.
6. Hamdi W, Ogawara H, Handa H, Tsukamoto N, Nojima Y, Murakami H. Clinical significance of regulatory T cells in patients with myelodysplastic syndrome. Eur J Haematol 2009; 82: 201–207.
7. Bouchliou I, Miltiades P, Nakou E, Spanoudakis E, Goutzouvelidis A, Vakalopoulou S, et al. Th17 and Foxp3(+) T regulatory cell dynamics and distribution in myelodysplastic syndromes. Clin Immunol 2011; 139: 350–359.
8. Fujimura T, Kambayashi Y, Aiba S. The expression of CD39/Entpd1 on granuloma composing cells and induction of Foxp3+ regulatory T cells in sarcoidosis. Clin Exp Dermatol 2012 (in press).
9. Wakusawa C, Fujimura T, Kambayashi Y, Hashimoto A, Aiba S. Pigmented necrobiosis lipoidica accompanied by insulin dependent diabetes mellitus induces CD163 positive proinflammatory macrophages and IL-17 producing cells. Acta Derm Venereol 2013; 93: 475–476.
10. Wakusawa C, Fujimura T, Haga T, Aiba S. Granulomatous pigmented purpuric dermatitis associated with primary Sjogren's syndrome. Acta Derm Venereol 2012; 92: 95–96.
11. Fujimura T, Kambayashi Y, Hidaka T, Hashimoto A, Haga T, Aiba S. Comparison of Foxp3+ regulatory T-cells and CD163+ macrophages in invasive and non-invesive extramammary Paget's disease. Acta Derm Venereol 2012; 92: 625–628.
12. Satoh T, Takeuchi O, Vandenbon A, Yasuda K, Tanaka Y, Kumagai Y, et al. The Jmjd3-Irf4 axis regulates M2 macrophage polarization and host responses against helminth infection. Nat Immunol 2010; 11: 936–944.
13. Fujimura T, Ring S, Umansky V, Mahnke K, Enk AH. Regulatory T cells (Treg) stimulate B7-H1 expression in myeloid derived suppressor cells (MDSC) in ret melanomas. J Invest Dermatol 2012; 132: 1239–1246.

Toxicology in Vitro 28 (2014) 759–768

Contents lists available at ScienceDirect

Toxicology in Vitro

journal homepage: www.elsevier.com/locate/toxinvit

Evaluation of the Multi-ImmunoTox Assay composed of 3 human cytokine reporter cells by examining immunological effects of drugs

Yutaka Kimura, Chizu Fujimura, Yumiko Ito, Toshiya Takahashi, Setsuya Aiba *

Department of Dermatology, Tohoku University Graduate School of Medicine, Sendai 980-8574, Japan

ARTICLE INFO

Article history:
Received 18 November 2013
Accepted 24 February 2014
Available online 4 March 2014

Keywords:
Immunotoxicity
Reporter assay
Alternatives to animals

ABSTRACT

We established a luciferase reporter assay system, the Multi-ImmunoTox Assay (MITA), to evaluate the effects on key predictive *in vitro* components of the human immune system. The system is composed of 3 stable reporter cell lines transfected with 3 luciferase genes, SLG, SLO, and SLR, under the control of 4 cytokine promoters, IL-2, IFN-γ, IL-1β, and IL-8, and the G3PDH promoter. We first compared the effects of dexamethasone, cyclosporine, and tacrolimus on these cell lines stimulated with phorbol 12-myristate 13-acetate and ionomycin, or lipopolysaccharides, with those on mRNA expression by the mother cell lines and human whole blood cells after stimulation. The results demonstrated that MITA correctly reflected the change of mRNA of the mother cell lines and whole blood cells. Next, we evaluated other immunosuppressive drugs, off-label immunosuppressive drugs, and non-immunomodulatory drugs. Although MITA did not detect immunosuppressive effects of either alkylating agents or antimetabolites, it could demonstrate those of the off-label immunosuppressive drugs, sulfasalazine, chloroquine, minocycline, and nicotinamide. Compared with the published immunological effects of the drugs, these data suggest that MITA can present a novel high-throughput approach to detect immunological effects of chemicals other than those that induce immunosuppressive effects through their inhibitory action on cell division.

1. Introduction

Environmental contaminants, food additives, and drugs can target the immune system, resulting in adverse health effects, such as the development of allergies, autoimmune disorders, cancers, and other diseases. Accordingly, immunotoxicity, which is defined as the toxicological effects of xenobiotics on the functioning of the immune system, has raised serious concerns from the public as well as regulatory agencies. Currently, the assessment of chemical immunotoxicity relies on animal models and assays that characterize immunosuppression and sensitization. However, animal studies have many drawbacks, such as expense, ethical concerns, and eventual relevance to risk assessment for humans. Therefore, European policy is promoting alternative testing methods and assessment strategies to reduce the use of laboratory animals and, if possible, replace animals employed for scientific studies (Balls et al., 1995).

A workshop hosted by the European Centre for the Validation of Alternative Methods (ECVAM) in 2003 focused on state-of-the-art *in vitro* systems for evaluating immunotoxicity (Galbiati et al., 2010; Gennari et al., 2005; Lankveld et al., 2010). In that workshop, a tiered approach was proposed, since useful information can be obtained from regular 28-day general toxicity tests. Namely, prescreening for direct immunotoxicity starts with the evaluation of myelotoxicity. Compounds that are capable of damaging or destroying the bone marrow will most likely have immunotoxic effects. If compounds are not potentially myelotoxic, they are tested for lymphotoxicity. Then, they are tested for immunotoxicity by approaches such as human whole-blood cytokine release assay (HWBCRA), lymphocyte proliferation assay, mixed lymphocyte reaction, natural killer cell assay, T-cell-dependent antibody response, dendritic cell maturation, and fluorescent cell chip. Among these assays, HWBCRA has undergone formal prevalidation, although other techniques are being examined or have been previously examined in a rigorous prevalidation effort by ECVAM and other groups.

The principle of HWBCRA, described by Langezaal et al. (2002), is based on the well-known human whole-blood method for pyrogen testing (Hartung, 2002). In brief, human blood is treated with lipopolysaccharide (LPS) or staphylococcal enterotoxin B (SEB),

* Corresponding author. Address: Department of Dermatology, Tohoku University Graduate School of Medicine, 1-1 Seiryo-machi, Sendai 980-8574, Japan. Tel./fax: +81 22 717 7271.
E-mail address: saiba@med.tohoku.ac.jp (S. Aiba).

http://dx.doi.org/10.1016/j.tiv.2014.02.013
0887-2333/

which causes monocytes and Th2 lymphocytes to produce IL-1β and IL-4, respectively. After incubation for 40 h in the presence or absence of immunotoxic and non-immunotoxic test compounds, the levels of IL-1β and IL-4 in the supernatant are quantified, and the 50% inhibitory concentration (IC50) and the fourfold stimulating concentration (SC4) are calculated to establish the immunotoxic potency (Langezaal et al., 2002). According to the EC-VAM workshop, this method has several advantages, such as the avoidance of species differences between humans and animals, employment of human primary cells, simple culture techniques, and reduced expense and time requirements as compared to animal experiments. The interindividual variation in leukocyte numbers and their response to stimuli is a major concern when using HWBCRA. Although cryopreservation techniques for human whole blood can overcome these problems (Schindler and Hartung, 2002), this method is not suitable as a high-throughput assay to evaluate vast numbers of chemicals.

In the present study, to develop a high-throughput screening system to evaluate chemical immunotoxicity, we first established 3 stable reporter cell lines transfected with luciferase genes under the control of IL-2, IFN-γ, IL-8, and IL-1β promoters. We selected these 4 cytokines because IL-2 and IFN-γ are mainly produced by T cells and reflect T-cell function, while IL-8 and IL-1β are mostly produced by monocytes or dendritic cells and correspond with their activity. Next, we examined the effects of 3 well-characterized immunosuppressive drugs, dexamethasone (Dex), cyclosporine A (CyA), and tacrolimus (Tac), on luciferase activities of these three cell lines stimulated with phorbol 12-myristate 13-acetate (PMA) and ionomycin (Io) or lipopolysaccharide (LPS). Then, we compared the results with their effects on mRNA expression by the mother cell lines, Jurkat cells or THP-1 cells, under the relevant stimulation. Furthermore, we also compared their effects on luciferase activities with mRNA expression by human whole blood cells stimulated with PMA/Io or LPS in the presence of these immunosuppressive drugs. Finally, we treated these cell lines with immunosuppressive drugs, immunomodulatory drugs, or drugs without known immunomodulatory effects and estimated the performance of our screening system for immunotoxicity.

2. Materials and methods

2.1. Reagents

Water-soluble dexamethasone (Dex), cyclosporin A (CyA), tacrolimus (FK-506), rapamycin, cyclophosphamide (CP), azathioprine (AZ), mycophenolic acid (MPA), mizoribine (MZR), methotrexate (MTX), sulfasalazine (SASP), colchicine, chloroquine (CQ), minocycline (MC), nicotinamide (NA), acetaminophen (AA), digoxin, warfarin, phorbol 12-myristate 13-acetate (PMA), ionomycin (Io), and lipopolysaccharides from E. coli 026:B6 (LPS) were purchased from Sigma–Aldrich (St. Louis, MO).

2.2. Cell lines and reporter cell lines

The human acute T lymphoblastic leukemia cell line Jurkat and the human acute monocytic leukemia cell line THP-1 (ATCC, Manassas, VA) were cultured in RPMI-1640 (Gibco, Carlsbad, CA) with antibiotic–antimycotic (Invitrogen, Carlsbad, CA) and 10% fetal calf serum (Biological Industries, Kibbutz Beit Haemek, Israel) (Growth medium) at 37 °C with 5% CO_2. We previously established 2 reporter cell lines, #2H4 derived from Jurkat cells containing stable luciferase green (SLG) regulated by IL-2 promoter, stable luciferase orange (SLO) regulated by IFN-γ promoter, and stable luciferase red (SLR) regulated by G3PDH promoter (Saito et al., 2011) and THP-G8 cells derived from THP-1 cells containing SLO regulated by IL-8 promoter and SLR regulated by G3PDH promoter (Takahashi et al., 2011).

In the present study, we further established THP-G1b cells derived from THP-1 cells containing SLG regulated by IL-1β promoter and SLR by G3PDH promoter. Full details are available in Supplementary Methods.

2.3. Chemical treatment

Based on the previous reports (Saito et al., 2011; Takahashi et al., 2011), #2H4 cells (2×10^5 cells/50 μl/well), THP-G1b cells, or THP-G8 cells (5×10^4 cells/50 μl/well) in 96-well black plates (Greiner bio-one GmbH, Frickenhausen, Germany) were pretreated with different concentrations of chemicals for 1 h. The optimum cell numbers at seeding were based on the previous reports. Afterwards, #2H4 cells were stimulated with 25 nM of PMA and 1 μM of ionomycin (PMA/Io) for 6 h, while THP-G1b cells or THP-G8 cells were stimulated with 100 ng/ml of LPS for 6 h. In some experiments, we changed the stimulation time to determine the optimum incubation period for the luciferase assay. Three luciferase activities, SLG luciferase activity (SLG-LA), SLO luciferase activity (SLO-LA), and SLR luciferase activity (SLR-LA), were simultaneously determined by using a microplate-type luminometer with a multicolor detection system, Phelios (Atto Co., Tokyo, Japan), and the Tripluc luciferase assay reagent (TOYOBO) according to the manufacturer's instructions. To rule out the variation of cell number or cell viability after chemical treatment, we obtained normalized luciferase activity as follows:

Normalized SLG-LA (nSLG-LA) or normalized SLO-LA (nSLO-LA) = SLG-LA or SLO-LA/SLR-LA.

We also calculated percent suppression as follows:

% suppression = (1 − nSLG-LA or nSLO-LA of the reporter cells treated with drugs/nSLG-LA or nSLO-LA of non-treated reporter cells) × 100.

To eliminate the data affected by cytotoxic effects of drugs or cell death, we also defined the inhibition index of SLR-LA (II-SLR-LA) as follows:

II-SLR-LA = SLR-LA of reporter cells that were treated with chemicals/SLR-LA of untreated reporter cells.

Since our previous study has reported that, in the treatment showing more than 5% in II-SLR-LA, more than 75% of cells are PI-excluding living cells (Takahashi et al., 2011), we presented only the data that demonstrated more than 5% in II-SLR-LA in this study.

2.4. Human whole-blood cytokine mRNA expression test (HWBCMET)

The human whole-blood cytokine mRNA expression test (HWBCMET) was performed by modifying the HWBCRA protocol by Langezaal et al. (2002)) and Thurm and Halsey (2005). The following studies were approved by the ethics committee of Tohoku University Graduate School of Medicine, Sendai, Japan, and conducted according to the Declaration of Helsinki principles. Full details are available in Supplementary Methods.

2.5. mRNA expression by Jurkat and THP-1 cells

Jurkat or THP-1 cells (3×10^6 cells) in 6-well plates were pretreated with different concentrations of drugs for 1 h and then stimulated with PMA/Io or LPS for 6 h, respectively. Total RNA was extracted by using Isogen (Nippon Gene, Tokyo, Japan) according to the manufacturer's instructions. The total RNA concentration was measured by using a NanoDrop spectrophotometer.

2.6. Quantitative RT-PCR

Complementary DNAs (cDNAs) were synthesized by using the TaKaRa RNA PCR Kit (AMV) (Takara Bio Inc., Otsu, Japan) according to the manufacturer's instructions. Quantitative real-time PCR (qPCR) was performed by using the Mx3000p QPCR System (Stratagene; Agilent Technologies Division, Santa Clara, CA). Sequences for each target gene were obtained from GenBank. Forward and reverse primers and TaqMan probes were selected by Primer Express 1.0 (Applied Biosystems) and synthesized by SIGMA GENOSYS (Ishikari, Japan). Each primer and TaqMan probe set used is described in our previous publication (Saito et al., 2011). qPCR reaction mixtures (25 μl) contained 10 ng of template cDNA, 400 nM of forward and reverse primers, 60 nM TaqMan probe, 30 nM ROX, and Brilliant II Fast QPCR Master Mix (Stratagene; Agilent Technologies Division). The thermal cycling conditions were 2 min for polymerase activation and cDNA denaturation at 95 °C and 45 cycles of 95 °C for 5 s and 60 °C for 20 s. Constitutively expressed G3PDH served as a normalization control by using the ΔΔCt method (Livak and Schmittgen, 2001). In the examination of mRNA from whole blood cells, percent suppression was calculated as follows:

% suppression = (1 − the normalized mRNA expression of WBC in the presence of drugs/the normalized mRNA expression of WBC in the absence of drugs) × 100.

2.7. Statistics

Representative data from at least three independent experiments for each analysis is shown. For each experiment, a one-way ANOVA test followed by Dunnett's post hoc test was used to evaluate statistical significance. For comparison of three independent experiments, the Student's *t*-test was used to evaluate statistical significance. *p* values <0.05 were considered statistically significant.

3. Results

3.1. Three reporter cell lines, #2H4, THP-G1b, and THP-G8, responded with relevant stimulations by augmenting their SLG-LA or SLO-LA

First, we stimulated #2H4 cells with PMA/Io and THP-G1b or THP-G8 cells with LPS and measured SLG-LA, SLO-LA, and SLR-LA after stimulation. PMA/Io significantly augmented SLG(IL2)-LA and SLO(IFN)-LA of #2H4 cells corresponding with IL-2 and IFN-γ promoter activities, respectively, from 6 h after stimulation, while it suppressed SLR(G3PDH)-LA corresponding with G3PDH promoter activity (Fig. 1A). Similarly, LPS significantly augmented SLG(IL1)-LA of THP-G1b cells corresponding with IL-1β promoter activity and SLO(IL8)-LA of THP-G8 cells corresponding with IL-8 promoter activity without affecting SLR(G3PDH)-LA of both cell lines from 3 h after stimulation (Fig. 1B and C). In Fig. 1A, B, and C, we also presented nSLG(IL2)-LA and nSLO(IFN)-LA of #2H4 cells, nSLG(IL1)-LA of THP-G1b cells, and nSLO-LA(IL8) of THP-G8 cells at various time periods after stimulation. PMA/Io significantly and time-dependently augmented both nSLG(IL2)-LA and nSLO(IFN)-LA of #2H4 cells from 6 to 10 h after stimulation. On the other hand, LPS significantly and time-dependently augmented nSLG(IL1)-LA of THP-G1b cells from 4 to 9 h after stimulation, while it significantly augmented nSLO(IL8)-LA of THP-G8 cells from 3 to 10 h after stimulation, with maximum induction at 5 h.

3.2. The effects of 3 immunosuppressive drugs on the reporter activity of the three reporter cells correlate with their effects on mRNA expression by Jurkat or THP-1 cells

Next, we examined whether the effects of 3 well-characterized immunosuppressive drugs, Dex, CyA, and Tac, on nSLG-LA or nSLO-LA of 3 reporter cells stimulated with PMA/Io or LPS correlate with their effects on the corresponding mRNA expression by Jurkat or THP-1 cells (Fig. 2). When we stimulated #2H4 cells with PMA/Io in the presence of Dex, CyA or Tac, Dex significantly suppressed nSLG(IL2)-LA at concentrations of 0.01 μg/ml and greater (≥0.01 μg/ml) and nSLO(IFN)-LA at ≥100 μg/ml, while CyA suppressed nSLG(IL2)-LA at ≥0.03 ng/ml and nSLO(IFN)-LA at ≥0.001 μg/ml, and Tac suppressed nSLG(IL2)-LA and nSLO(IFN)-LA at ≥0.016 ng/ml. Although Dex suppressed nSLO(IFN)-LA, the concentration to decrease nSLO(IFN)-LA was greater than 100 μg/ml, and the magnitude of the suppression was small. When we stimulated THP-G1b cells with LPS in the presence of Dex, CyA, or Tac, Dex significantly suppressed nSLG(IL1)-LA at ≥0.01 μg/ml, but CyA and Tac did not. Similarly, when THP-G8 cells were stimulated with LPS in the presence of Dex, CyA, or Tac, only Dex significantly suppressed nSLO(IL8)-LA at ≥0.01 μg/ml.

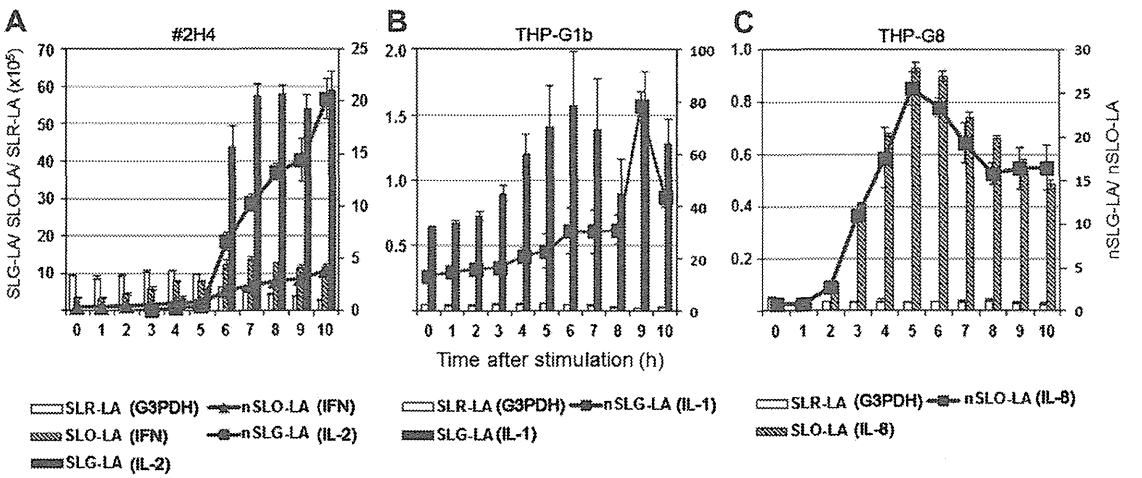

Fig. 1. Time course of IL-2, IFN-γ, IL-1β, and IL-8 reporter activities in PMA/Io-stimulated #2H4 cells and LPS-stimulated THP-G1b or THP-G8 cells. #2H4 cells (2×10^5 cells/100 μl/well) (A) in 96-well black plates were stimulated with PMA/Io, while THP-G1b (B) or THP-G8 cells (5×10^4 cells/100 μl/well) (C) were treated with LPS. Then, SLG-LA, SLO-LA, and SLR-LA were measured after stimulation by using a microplate-type luminometer with a multi-color detection system. To rule out the variation of cell number or cell viability after chemical treatment, normalized SLG luciferase activity (nSLG-LA) or SLO luciferase activity (nSLO-LA) was obtained by dividing SLG-LA or SLO-LA with SLR-LA. Data represent means +/− SD ($n = 4$). SLG-LA (IL-2), SLO-LA (IFN-γ), and SLR-LA (G3PDH) in A, SLG-LA (IL-1β) and SLR-LA (G3PDH) in B, and SLO-LA (IL-8) and SLR-LA (G3PDH) in C.

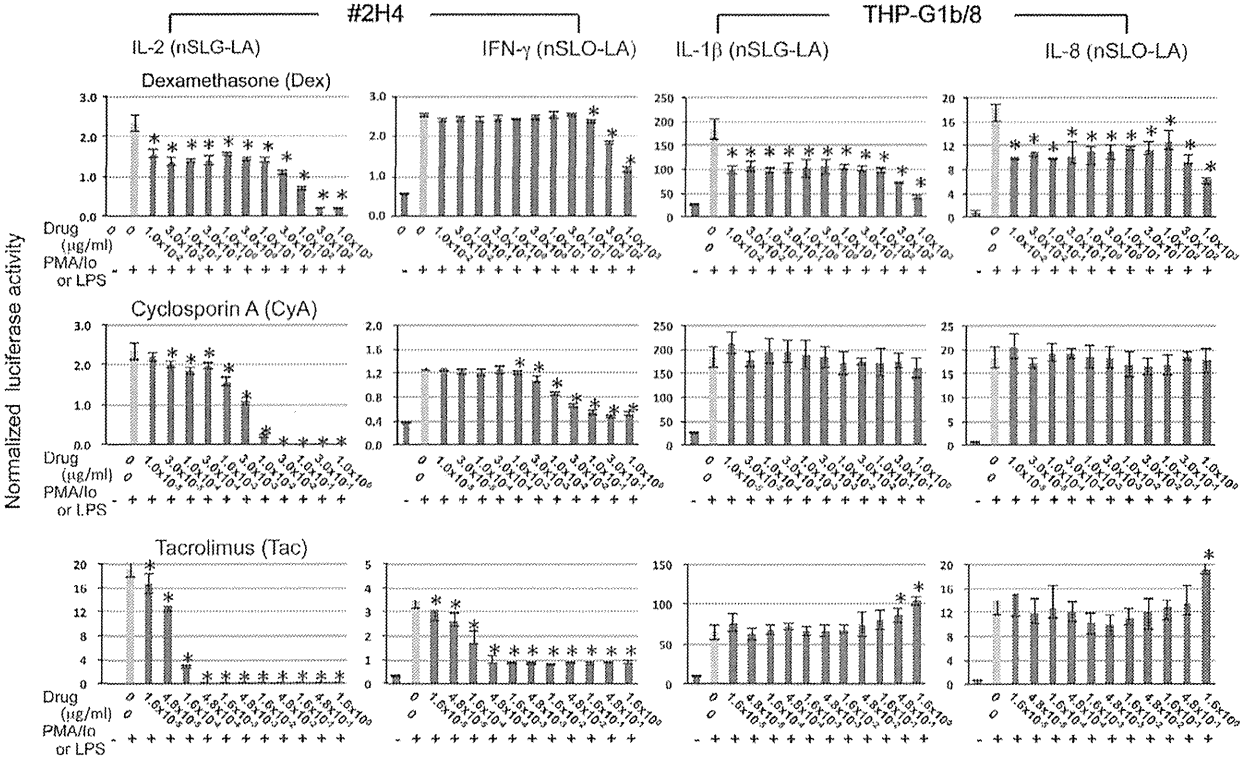

Fig. 2. The effects of Dex, CyA, and Tac on IL-2, IFN-γ, IL-1β, or IL-8 reporter activity of reporter cell lines after relevant stimulation. #2H4 cells, THP-G1b cells, or THP-G8 cells were pretreated with the indicated concentrations of drugs for 1 h and then stimulated with PMA/Io or LPS for 6 h. Luciferase activity was determined by using a microplate-type luminometer with a multi-color detection system. IL-2 and IFN-γ promoter activities are represented as nSLG-LA and nSLO-LA of #2H4 cells, respectively. IL-1β and IL-8 promoter activities are represented as nSLG-LA of THP-G1b and nSLO-LA of THP-G8 cells, respectively. Data represent means +/− SD ($n = 4$). * Means statistical significance ($p < 0.05$). Gray bars indicate the value for stimulation without drugs. These results are representative of three independent experiments.

Next, we stimulated the mother cell line of #2H4 cells, Jurkat cells, with PMA/Io in the presence of Dex, CyA, or Tac and the IL-2 or IFN-γ mRNA expression was examined by qPCR (Fig. 3). Dex suppressed only IL-2 mRNA expression at ⩾6 μg/ml, while both CyA and Tac suppressed IL-2 as well as IFN-γ mRNA expression at concentrations of ⩾0.012 μg/ml and 0.008 μg/ml, respectively. When the mother cell line of THP-G1b and THP-G8 cells, THP-1 cells, was stimulated with LPS in the presence of the three inhibitors, Dex significantly suppressed both IL-1β and IL-8 mRNA at the concentration of ⩾0.6 μg/ml, but CyA and Tac did not (Fig 3). These data indicate that the suppression profiles obtained by three reporter cell lines correlate closely with those obtained by qPCR analysis of mRNA expression by Jurkat cells or THP-1 cells. Thus, we designated the immunotoxicity assay using 3 reporter cell lines as Multi-ImmunoTox Assay (MITA).

3.3. The effects of 3 immunosuppressive drugs on mRNA expression by whole blood cells stimulated with PMA/Io or LPS also corresponded with their effects on the reporter activities of the 3 reporter cell lines

Next, we examined the correlation between HWBCRA and MITA. However, HWBCRA used SEB and LPS as stimulants and quantified IL-1β and IL-4 to characterize the immunotoxicity of chemicals. In contrast, MITA uses PMA/Io and LPS as stimulants and IL-2, IFN-γ, IL-1β, and IL-8 promoter activities as outputs. Therefore, we stimulated whole blood cells (WBC) from healthy volunteers with 25 nM of PMA and 1 μM of Io or 100 ng/ml LPS for 6 h in the presence or absence of 3 representative immunosuppressing drugs and analyzed IL-2, IFN-γ, IL-1β, and IL-8 mRNA by q PCR (HWBCMET). Fig. 4, which shows the % suppression of 3 drugs on the induction of mRNA for 4 cytokines in each individual, indicates that 1 μg/ml of Dex, 1 μg/ml of CyA, or 0.01 μg/ml of Tac significantly suppressed both IL-2 and IFN-γ mRNA induction after stimulation with PMA/Io, although the suppression by Dex was much smaller than that by CyA or Tac. On the other hand, only 1 μg/ml of Dex significantly suppressed IL-1β and IL-8 mRNA induction by WBC stimulated with LPS, while CyA and Tac did not. These data suggest that the evaluation of 3 immunosuppressive drugs by MITA corresponded well with that by HWBCMET, although the statistical analysis on MITA results could not detect the effects of Dex on IFN-γ reporter activity.

3.4. Several immunosuppressive drugs suppressed the reporter activity of the 3 reporter cell lines at concentrations equal to or less than 5 × Cmax

Based on these results, we evaluated other immunosuppressive or immunomodulatory drugs by using the 3 reporter cell lines. In Table 1, we present the results of immunosuppressive drugs classified by their principal mechanism (reviewed by Allison (2000)). Dex regulates gene expression; CyA, Tac, and RPM inhibit kinase or phosphatase; CP alkylates DNA; AZ, MPA, and MZR inhibit de novo purine synthesis; and MTX inhibits pyrimidine and purine synthesis.

We conducted 3 independent experiments for each drug and determined in each experiment whether chemicals induce statistically significant suppression or augmentation at two concentration ranges, equal or less than 5 × Cmax (⩽5 × Cmax) and greater than 5 × Cmax (>5 × Cmax). Cmax is defined as the peak plasma concentration of each drug after administration. Cmax of each drug

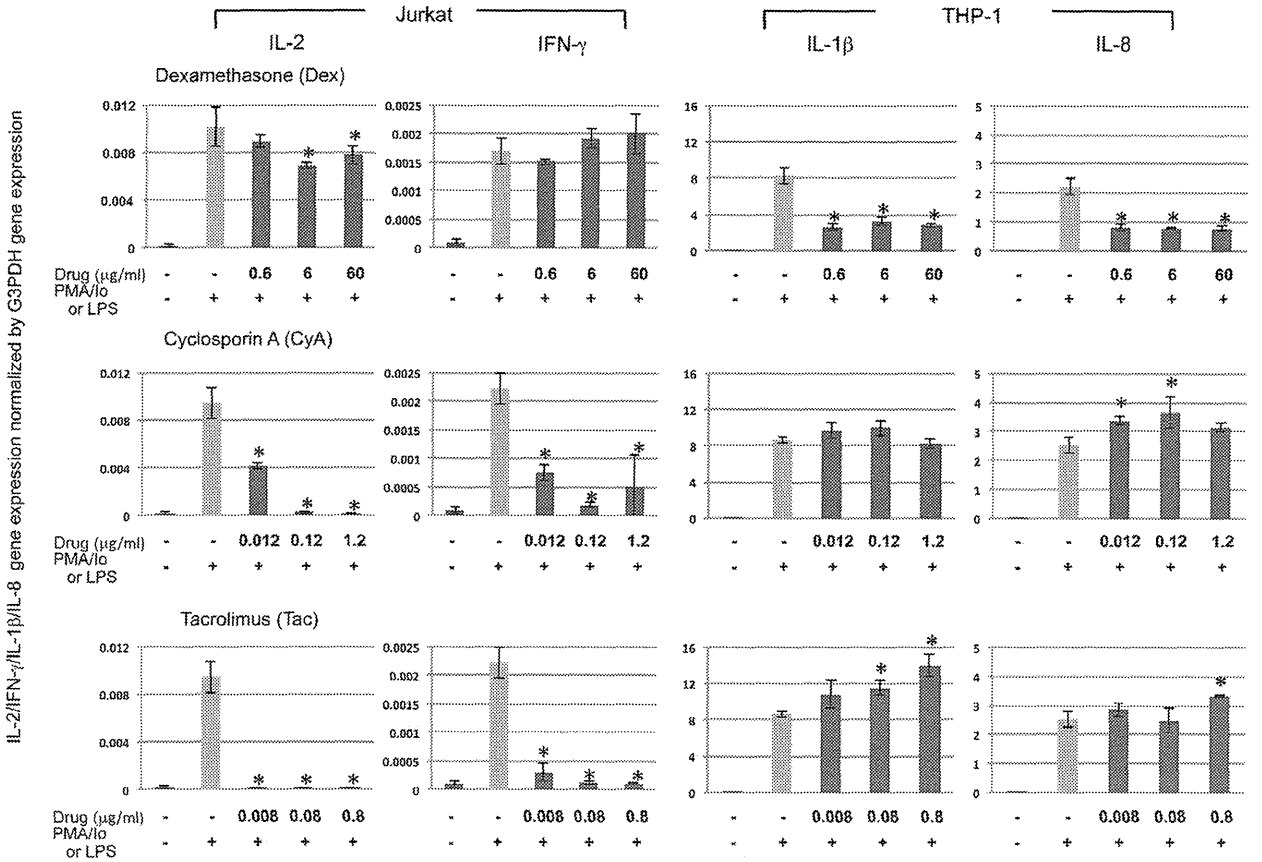

Fig. 3. The effects of Dex, CyA, and Tac on mRNA expression of IL-2 and IFN-γ by Jurkat cells and that of IL-1β and IL-8 by THP-1 cells after stimulation. Jurkat cells or THP-1 cells (3×10^6 cells/well) in 6-well plates were pretreated with different concentrations of drugs for 1 h, followed by stimulation with PMA/Io or LPS for 6 h, respectively. Then, mRNA expression of the indicated genes was analyzed by qPCR. The gene expressions were normalized by G3PDH gene expression. Data represent means +/− SD ($n = 3$). * Means statistical significance ($p < 0.05$). Gray bars indicate the value for stimulation without drugs.

is shown along with dose and route of administration in Table S1. Since the drug concentration of interstitial fluid can be higher than that of blood in some drugs (Kiang et al., 2012; Wiskirchen et al., 2011) and Cmax is variable among subjects, we evaluated drugs in these two different concentration ranges, considering that if a drug suppresses or augments cytokine reporter activities at $\leqslant 5 \times$ Cmax, the observed effects can be expected in clinical use. On the other hand, when the effects are recognized only at $>5 \times$ Cmax, the drug potentially has immunomodulatory effects, which are not expected in clinical use. Statistically significant suppression is shown as −, statistically significant augmentation as +, and no significance as 0; and a lack of data due to the inability to dissolve chemicals in solvents at the concentration of $5 \times$ Cmax is shown as ND.

Furthermore, since the statistical evaluation of the chemicals in each experiment was not necessarily consistent among three independent experiments, we conducted statistical analysis on the results of 3 independent experiments. If chemicals showed statistically significant immunosuppression or immunostimulation in 3 experiments, they were judged as immunosuppressive or immunostimulatory drugs, respectively. If chemicals showed statistically significant immunosuppression or immunostimulation in only 2 independent experiments, they were judged as potential immunosuppressive or immunostimulatory drugs, respectively. If not, they were judged as ineffective.

Then, for potential immunosuppressive or immunostimulatory drugs, we selected their percent suppression or percent augmentation (negative percent suppression) in three experiments that showed the most remarkable change, calculated their percent suppression or percent augmentation, and statistically compared suppression or augmentation of chemicals with that of vehicle control in three different experiments by the Student's *t*-test. Only when chemicals demonstrated statistical significance, they were judged as immunosuppressive or immunostimulatory, respectively. In Table 1, the final judgment of immunotoxicity of chemicals by MITA was indicated as S for immunosuppression, A for immunoaugmentation, and N for no effect.

As mentioned above, Dex significantly suppressed IL-2, IL-1β, and IL-8 reporter activities at any concentration ranges in at least 2 of 3 experiments and that of IFN-γ at $>5 \times$ Cmax in 2 of 3 experiments (Table 1). Among 3 kinase or phosphatase inhibitors, CyA and Tac suppressed IL-2 and IFN-γ reporter activities at $\leqslant 5 \times$ Cmax in 3 experiments, while rapamycin did not show any inhibitory effects on IL-2 or IFN-γ reporter activity, but rather augmented IL-2 reporter activity at $\leqslant 5 \times$ Cmax in 2 of 3 experiments and IL-1β reporter activity at $>5 \times$ Cmax in 3 experiments (Table 1). In addition to the evaluations in which 3 out of 3 experiments demonstrated consistent results, the statistical analysis on the examinations in which only 2 out of 3 experiments demonstrated consistent results showed significant suppression in IL-1β reporter activity by Dex at $\leqslant 5 \times$ Cmax and significant augmentation in IL-2 reporter activity by RPM at both concentrations.

Among an alkylating agent, inhibitors of de novo purine synthesis, and an inhibitor of pyrimidine and purine synthesis (Table 1), none of the drugs except for AZ demonstrated immunosuppressive effects at any concentration ranges. Only AZ significantly suppressed

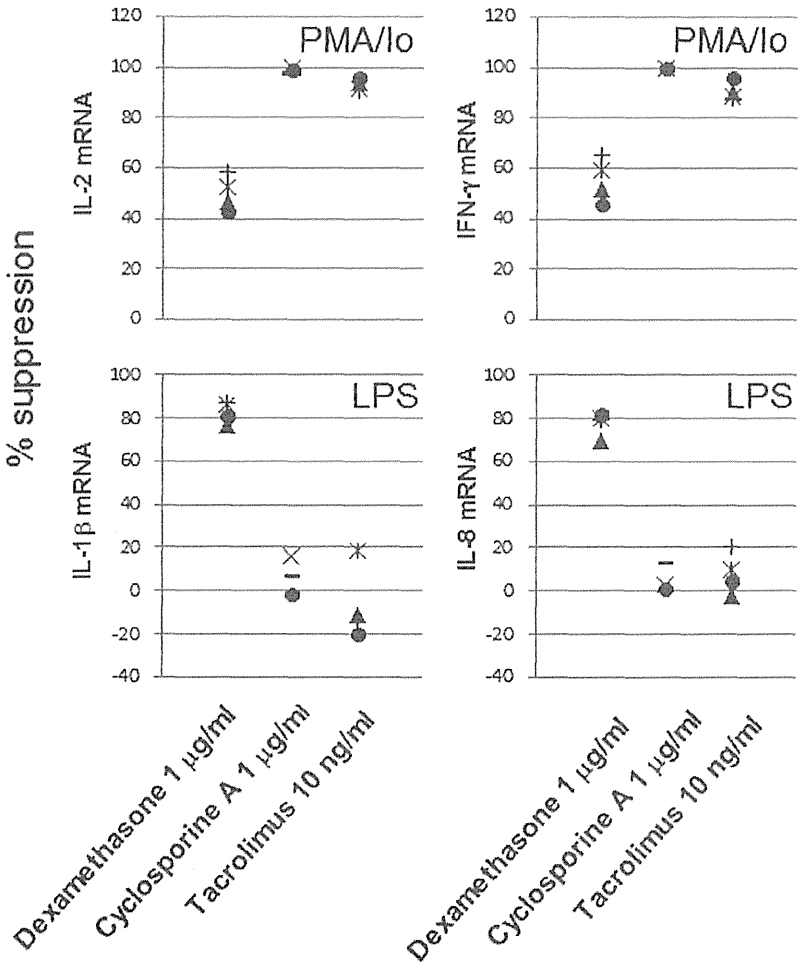

Fig. 4. The effects of Dex, CyA, and Tac on IL-2, IFN-γ, IL-1β, or IL-8 mRNA expression of whole blood cells stimulated with PMA/Io or LPS. Whole blood cells (WBC) from 6 healthy volunteers were collected using sodium heparin anti-coagulant and then diluted 1:2 with RPMI 1640 medium. Two ml of aliquots was either untreated or treated with 1 μg/ml of Dex, or 1 μg/ml of CyA or 10 ng/ml of Tac for 1 h. Then, the WBC were stimulated with PMA/Io or LPS for 6 h at 37 °C. The mRNA expression of indicated genes was analyzed by qPCR. The gene expressions were normalized by G3PDH gene expression. Percent suppression was calculated as described in Section 2. The percent suppression of drugs in each individual is plotted. Each symbol indicates a different individual.

IL-8 reporter activities at >5 × Cmax in 2 of 3 experiments. On the other hand, MPA significantly augmented IL-2 and IFN-γ reporter activities at ⩽5 × Cmax in 3 experiments. MZR increased all reporter activities at any concentration ranges in at least 2 of 3 experiments. In addition, CP augmented IFN-γ reporter activity at >5 × Cmax in 3 experiments, while MTX augmented IL-2 and IFN-γ reporter activities at any concentration ranges in 2 of 3 experiments. The statistical analysis on the examinations in which only 2 out of 3 experiments demonstrated consistent results showed significant augmentation in IL-1β reporter activity by AZ at >5 × Cmax, IL-2 reporter activity by MTX at >5 × Cmax, and IFN-γ reporter activity by MTX at both concentrations.

3.5. Sulfasalazine and nicotinamide significantly suppressed IL-1β and IL-8 reporter activities

Next, we examined the effects of drugs that are not classified as immunosuppressive or immunomodulatory drugs, but are currently in off-label use for the treatment of autoimmune or inflammatory disorders (Capell and Madhok, 2008; Chaiamnuay and Alarcon, 2008; Sturrock, 2008; Surjana and Damian, 2011) (Fig. 5 and Table 1). Among 5 off-label immunosuppressive drugs, SASP significantly suppressed 4 reporter activities at any concentration ranges in at least 2 of 3 experiments. CQ significantly suppressed IL-2 and IFN-γ reporter activities at any concentration ranges in at least 2 of 3 experiments, while it significantly suppressed IL-1β and IL-8 at >5 × Cmax in 3 experiments. MC significantly suppressed IL-2 and IFN-γ reporter activities at any concentration ranges in 3 experiments, while it did not affect IL-1β and IL-8 reporter activities. NA significantly suppressed IL-1β and IL-8 reporter activities at any concentrations in 3 experiments, while it augmented IL-2 and IFN-γ reporter activities at any concentrations in at least 2 of 3 experiments. Colchicine increased IL-1β reporter activity at ⩽5 × Cmax in 2 of 3 experiments and all reporter activities at >5 × Cmax in 3 experiments. The statistical analysis of the examinations in which only 2 out of 3 experiments demonstrated consistent results showed significant augmentation in IL-1β reporter activity by colchicine at ⩽5 × Cmax.

3.6. Two non-immunological drugs, warfarin and digoxin, suppressed some reporter activities at concentrations of ⩽5 × Cmax

We examined the effects of 3 non-immunological drugs on the reporter activities of the three reporter cell lines (Fig. 6 and Table 1). Warfarin suppressed IL-1β and IL-8 reporter activities at ⩽5 × Cmax in 2 of 3 experiments, while it augmented IL-2 and

Table 1
Summary of MITA for 9 immunosuppressive drugs, 5 off-label immunosuppressive drugs, and 3 non-immunomodulatory drugs.

Principal mechanism of action		Cmax	IL-2			IFN-γ			IL-1β			IL-8		
			⩽5 × Cmax	>5 × Cmax		⩽5 × Cmax	>5 × Cmax		⩽ × Cmax	>5 × Cmax		⩽5 × Cmax	>5 × Cmax	
Immunosuppressing drugs														
Regulation of gene expression	Dexamethasone (Dex)	88 ng/ml	−/−/−	S −/−/−	S	−/0/0	N −/+/−	N	−/−/−	S −/−/−	S	−/−/0*	S −/−/−	S
Kinase and phosphatase inhibitors	Cyclosporin A (CyA)	2144 μg/ml	−/−/−	S ND/ND/ND		−/−/−	S ND/ND/ND		0/0/0	N ND/ND/ND		0/−/0	N ND/ND/ND	
	Tacrolimus (Tac)	44.6 ng/ml	−/−/−	S −/−/−	S	−/−/−	S −/−/−	S	+/0/0	N 0/+/0	N	−/0/0	N 0/+/0	N
	Rapamycin (RPM)	4.0 ng/ml	0/+/+*	A 0/+/+*	A	0/−/0	N 0/0/0	N	0/0/0	N +/+/+	A	0/0/0	N 0/0/0	N
Alkylation	Cyclophosphamide (CP)	6.36 μg/ml	+/0/−	N 0/0/−	N	+/0/−	N +/+/+	A	0/0/−	N 0/0/−	N	0/0/−	N 0/+/−	N
Inhibition of de novo purine synthesis	Azathioprine (AZ)	73.7 ng/ml	0/0/0	N 0/−/−	N	0/0/0	N +/+/+	A	0/0/0	N +/−/+*	A	0/0/0	N +/−/−	N
	Mycophenolic acid (MPA)	34.0 μg/ml	+/+/+	A ND/ND/ND		+/+/+	A ND/ND/ND		0/0/+	N ND/ND/ND		0/0/0	N ND/ND/ND	
	Mizoribine (MZR)	9.6 μg/ml	+/+/−	N +/+/0	N	+/+/−	N +/0/+	N	+/+/+	A +/+/+	A	+/+/+	A +/+/+	A
Inhibition of pyrimidine and purine synthesis	Methotrexate (MTX)	162.2 ng/ml	+/0/+	N +/0/+*	A	0/+/+*	A 0/+/+*	A	0/0/−	N 0/0/−	N	0/0/−	N 0/0/−	N
Off-label immunosuppressing drugs														
	Sulfasalazine (SASP)	15.6 μg/ml	+/−/−	N −/−/−	S	−/−/−	S −/−/−	S	−/−/−	S −/−/−	S	−/−/−	S −/−/−	S
	Colchicine	5.64 ng/ml	0/0/0	N +/+/+	A	0/+/0	N +/+/+	A	+/0/+*	A +/+/+	A	+/0/0	N +/+/+	A
	Chloroquine (CQ)	555 ng/ml	−/−/−	S −/−/−	S	−/−/0	N −/−/−	S	0/0/0	N −/−/−	S	0/0/0	N −/−/−	S
	Minocycline (MC)	4.8 μg/ml	−/−/−	S −/−/−	S	−/−/−	S −/−/−	S	0/0/0	N 0/0/0	N	0/0/0	N 0/0/+	N
	Nicotinamide (NA)	22.4–26.3 μg/ml	+/−/+	N +/+/+	A	0/+/+	N +/+/+	A	−/−/−	S −/−/−	S	−/−/−	S −/−/−	S
Non-immunomodulatory drugs														
	Acetaminophen (AA)	9.4 ng/ml	+/+/+	A +/+/+	A	+/+/+	A +/+/+	A	+/0/0	N +/+/+	A	+/0/0	N +/+/+	A
	Digoxin	2.92 ng/ml	−/0/−	N −/−/−	S	0/0/−	N −/−/−	S	0/0/0	N +/0/0	N	0/0/0	N +/0/0	N
	Warfarin	685 μg/ml	+/+/+	A ND/ND/ND		0/+/+	N ND/ND/ND		−/0/*	S ND/ND/ND		−/−/0*	S ND/ND/ND	

− and + mean significant suppression and augmentation by one-way ANOVA followed by a Dunnett's post hoc test compared with the control group, respectively. 0 means no significant change.
* Means statistical significance by Student's t test S, A, and N indicate immunosuppression, immunoaugmentation, and no effect in final judgment, respectively.

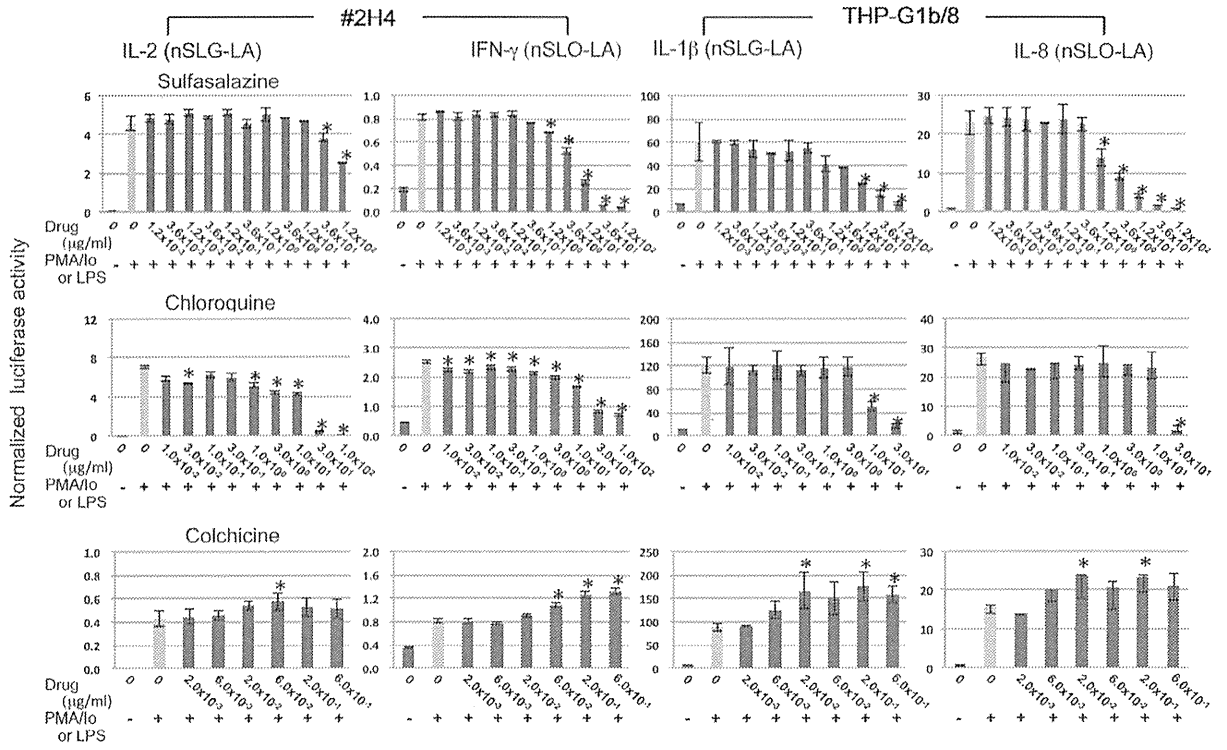

Fig. 5. The effects of SASP, CQ, and colchicine on IL-2, IFN-γ, IL-1β, or IL-8 reporter activity of reporter cell lines after relevant stimulation. #2H4 cells, THP-G1b cells, or THP-G8 cells were pretreated with the indicated concentrations of drugs for 1 h and then stimulated with PMA/Io or LPS for 6 h. Luciferase activity was determined by using a microplate-type luminometer with a multi-color detection system. Data represent means +/− SD ($n = 4$). * Means statistical significance ($p < 0.05$). Gray bars indicate the value for stimulation without drugs. These results are representative of three independent experiments.

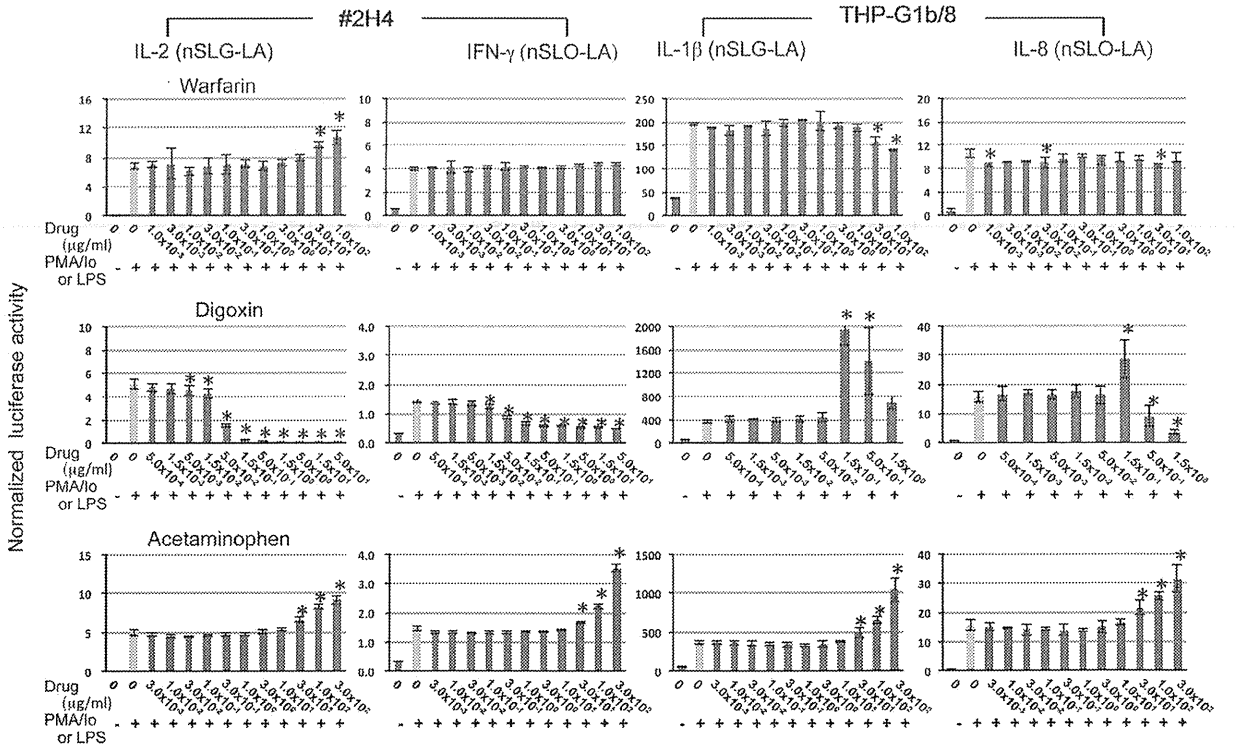

Fig. 6. The effects of warfarin, digoxin, and AA on IL-2, IFN-γ, IL-1β, or IL-8 reporter activity of reporter cell lines after relevant stimulation. #2H4 cells, THP-G1b cells, or THP-G8 cells were pretreated with the indicated concentrations of drugs for 1 h and then stimulated with PMA/Io or LPS for 6 h. Luciferase activity was determined by using a microplate-type luminometer with a multi-color detection system. Data represent means +/− SD ($n = 4$). * Means statistical significance ($p < 0.05$). Gray bars indicate the value for stimulation without drugs. These results are representative of three independent experiments.